RSC Advances

PAPER

View Article Online
View Journal | View Issue

Cite this: *RSC Adv.*, 2024, **14**, 23853

Unveiling the potential of novel indol-3-yl-phenyl allylidene hydrazine carboximidamide derivatives as AChE/BACE 1 dual inhibitors: a combined *in silico*, synthesis and *in vitro* study†

Amit Sharma,[a] Santosh Rudrawar,[bc] Ankita Sharma,[d] Sandip B. Bharate[d] and Hemant R. Jadhav *[a]

Received 13th June 2024
Accepted 23rd July 2024

DOI: 10.1039/d4ra04315d

rsc.li/rsc-advances

Considering the failure of many enzyme inhibitors for Alzheimer's disease (AD), research is now focused on multi-target directed drug discovery. In this paper, inhibition of two essential enzymes implicated in AD pathologies, acetylcholinesterase (AChE) and BACE 1 (Beta-site APP Cleaving Enzyme), has been explored. Taking clues from our previous work, 41 novel indol-3-yl phenyl allylidene hydrazine carboximidamide derivatives were synthesized. The results indicated that compounds inhibited both enzymes in micromolar concentrations. Compound **1l** is proposed as the most active. *In silico*, it was seen to occupy the binding pocket of AChE and BACE 1. The ADME predictions showed that these compounds have acceptable physicochemical characteristics. This study provides new leads for the assessment of AChE and BACE 1 dual inhibition as a promising strategy for AD treatment.

1. Introduction

Alzheimer's disease (AD) is a complex and debilitating neurological disorder that primarily affects the brain, leading to cognitive decline and memory loss. AD is a chronic and progressive disease that gradually impairs an individual's ability to function independently, affecting their daily activities and quality of life.[1] Worldwide, as of 2023, the current estimate of 50 million people worldwide with dementia is expected to increase to 78 million by 2030 and a staggering 139 million by 2050.[2] The disease is characterized by several neuropathological features such as reduced levels of acetylcholine (ACh), accumulation of amyloid-β, formation of neurofibrillary tangles made of hyperphosphorylated tau-protein, oxidative stress, and imbalanced biometal levels.[3] The current approach to treating neurological disorders involves the use of medication that aims to enhance cognitive functions or alleviate symptoms by targeting the mechanisms of neurotransmitters in the brain using cholinesterase inhibitors (such as donepezil, galantamine, and rivastigmine see Fig. 1) and *N*-methyl-D-aspartate (NMDA) receptor antagonist *i.e.* memantine.[4,5] Patients with declining cognitive functions who are prescribed cholinesterase inhibitors or similar medications have not shown any significant improvement in preventing the advancement of AD.[6] Despite ongoing efforts to develop drugs that modify the course of AD and slow its progression, there are still potential obstacles that may impede success, such as unanticipated toxicity or inadequate effectiveness in human clinical trials.[7] The complexity of AD and its multifaceted nature have rendered the existing single-targeted drugs ineffective in producing the desired therapeutic effect. It is widely believed that compounds with the ability to modulate multiple targets are more effective than those that only act on a single target, due to the inadequate results of the one drug one target (ODOT) strategy. Therefore, there is a need for the development of multi-targeted therapies to slow down the progression of the disease.[8,9]

The most effective approach, therefore, is to either combine multiple drugs that target different mechanisms or to use a single chemical compound that contains multiple pharmacophores, resulting in greater activity than the individual parent drugs.[10] Researchers tend to concentrate on adding multiple pharmacophores into a single drug to address the challenges associated with combining different drugs, such as drug resistance, drug–drug interactions, and to improve management of unresponsive AD patients. As a result, medicinal chemists are

[a]*Pharmaceutical Chemistry Research Laboratory, Department of Pharmacy, Birla Institute of Technology and Science Pilani, Pilani Campus, Vidya Vihar, Pilani – 333031, RJ, India. E-mail: hemantrj@pilani.bits-pilani.ac.in; Fax: +91-1596-244183; Tel: +91-1596-255 506*

[b]*The Institute for Biomedicine and Glycomics, Griffith University, Gold Coast 4222, Australia*

[c]*School of Pharmacy and Medical Sciences, Griffith University, Gold Coast 4222, Australia*

[d]*Natural Products and Medicinal Chemistry Division, CSIR-Indian Institute of Integrative Medicine, Canal Road, Jammu – 181110, India*

† Electronic supplementary information (ESI) available. See DOI: https://doi.org/10.1039/d4ra04315d

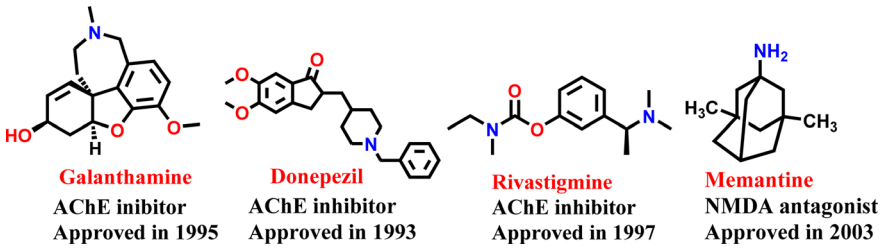

Fig. 1 US FDA approved drugs for the treatment of Alzheimer's disease.

developing drugs that can effectively act on multiple targets to treat AD.[11,12]

Numerous hypotheses have been put forward over time, each highlighting several molecular targets for addressing this disease.[13] Two widely accepted theories for AD are the cholinergic and amyloidogenic hypotheses.[14]

The primary reason behind the decrease in levels of the ACh neurotransmitter in the brain is the enzymatic activity of acetylcholinesterase (AChE), which breaks it down through hydrolysis. According to the cholinergic hypothesis, the decline in cognitive functions is linked to the decreased levels of ACh in the cholinergic synapses. It has been acknowledged that AChE plays a crucial role in promoting the buildup of Aβ aggregates in individuals with Alzheimer's disease. Moreover, *in vitro* research suggests that AChE may be responsible for triggering the formation of Aβ fibrils and plaques. However, further research has indicated that this factor alone cannot fully explain the development of AD.[15–18]

The accumulation of Aβ is a primary factor in the onset and progression of Alzheimer's disease. The formation of Aβ oligomers and plaques, which contribute to the pathology of Alzheimer's disease, is a result of the breakdown of the Aβ precursor protein (APP) *via* the amyloidogenic pathway.[19] By following the non-amyloidogenic pathway, the APP is broken down by α-secretase into soluble fragments that can be easily eliminated from the body. The amyloidogenic pathway involves the activity of β-secretase (also called Aβ precursor cleaving enzyme or BACE 1), which breaks down APP and leads to the formation of Aβ fragments that are insoluble and waxy in nature.[20,21] Targeting BACE 1 is crucial in the development of drugs for Alzheimer's disease. An essential target in the treatment of Alzheimer's disease is the inhibition of the spontaneous aggregation of amyloid β_{1-42} ($A\beta_{1-42}$), a protein that tends to aggregate on its own.[22]

The hypothesis resulted in the FDA's approval of aducanumab, an anti-amyloid monoclonal antibody, and the recently approved lecanemab, which target amyloid and are the only approved therapies for altering the progression of Alzheimer's disease. While the effectiveness of both the antibodies in slowing down the progression of Alzheimer's disease is still being debated, it has been shown to enhance memory and cognitive function impairments that are connected to Aβ plaques.[23] Therefore, the present work was undertaken to identify dual AChE and BACE1 inhibitor.

Our group had reported a novel class of allylidene hydrazine carboximidamide derivatives as potent BACE 1 inhibitors, having aminoguanidine substitution on 3 atom allyl linker with two aromatic groups on either side.[24] Using the same scaffold, a new series of pyrrol-2-yl-phenyl allylidene hydrazine carboximidamide was designed which showed good inhibition of both AChE and BACE. The compound shown in Fig. 2 exhibited IC_{50} values of 57.09 μM and 74.24 μM against AChE and BACE 1, respectively (unpublished results from our group).

Similarly, Zhao's group has recently synthesized and evaluated multifunctional activities of bivalent β-carboline derivatives with good AChE inhibitory activity with IC_{50} values of 97 ± 0.91 nM.[25,26] In recent times, Liao *et al.*, reported cinnamic acid–β-carboline hybrids exhibits inhibition of AChE with IC_{50} value of 21.29 μM, respectively.[27] Pachon-Angona *et al.*, in 2019, synthesized hybrids of indole–donepezil–chromone compounds inhibiting AChE with an IC_{50} value of 1.73 μM.[28]

Donepezil also has a benzyl substitution and has two aromatic rings separated by a linker. Considering these similarities, it was inferred that incorporating bicyclic ring such as indole could impart AChE inhibitor property. It is reported that *N*-benzylated heterocyclic fragments can bind the PAS site of AChE.[27] Therefore, *N*-benzyl indole was considered on one side of 3 carbon linker having guanidine substitution as could help the structure to interact with the catalytic sites of AChE as well as BACE 1 (Fig. 2). It was hypothesized that –NH group of guanidine could form a hydrogen bond with Asp 32 and Asp 228 (key amino acid of BACE 1), ring A and B to occupy the S1, S3 cavities of BACE 1, and occupancy of PAS by *N*-benzyl indole and PAS of AChE of other aromatic ring. Herein, this study of synthesis, and *in vitro* evaluation of indol-3-yl-phenyl allylidene hydrazine carboximidamide derivatives as potential dual inhibitors of AChE and BACE 1 is presented.

2. Results and discussion

2.1. Design of novel dual AChE/BACE 1 inhibitors

The examination of AChE's X-ray crystal structure (PDB ID: 4EY7) revealed the presence of two binding sub-sites, namely PAS (peripheral anionic site) and CAS (catalytic active site), that play a role in the binding of acetylcholine. The PAS is distinctly separated from the choline binding pocket, which is situated in the active site, while the CAS is thought to be similar to the catalytic sub-sites seen in other serine hydrolases. The active site of AChE is commonly described as an active site gorge because it contains a catalytic triad comprising Ser200, His440, and Glu327, located at the base of the pocket. Studies conducted through both kinetic and chemical analyses have suggested the

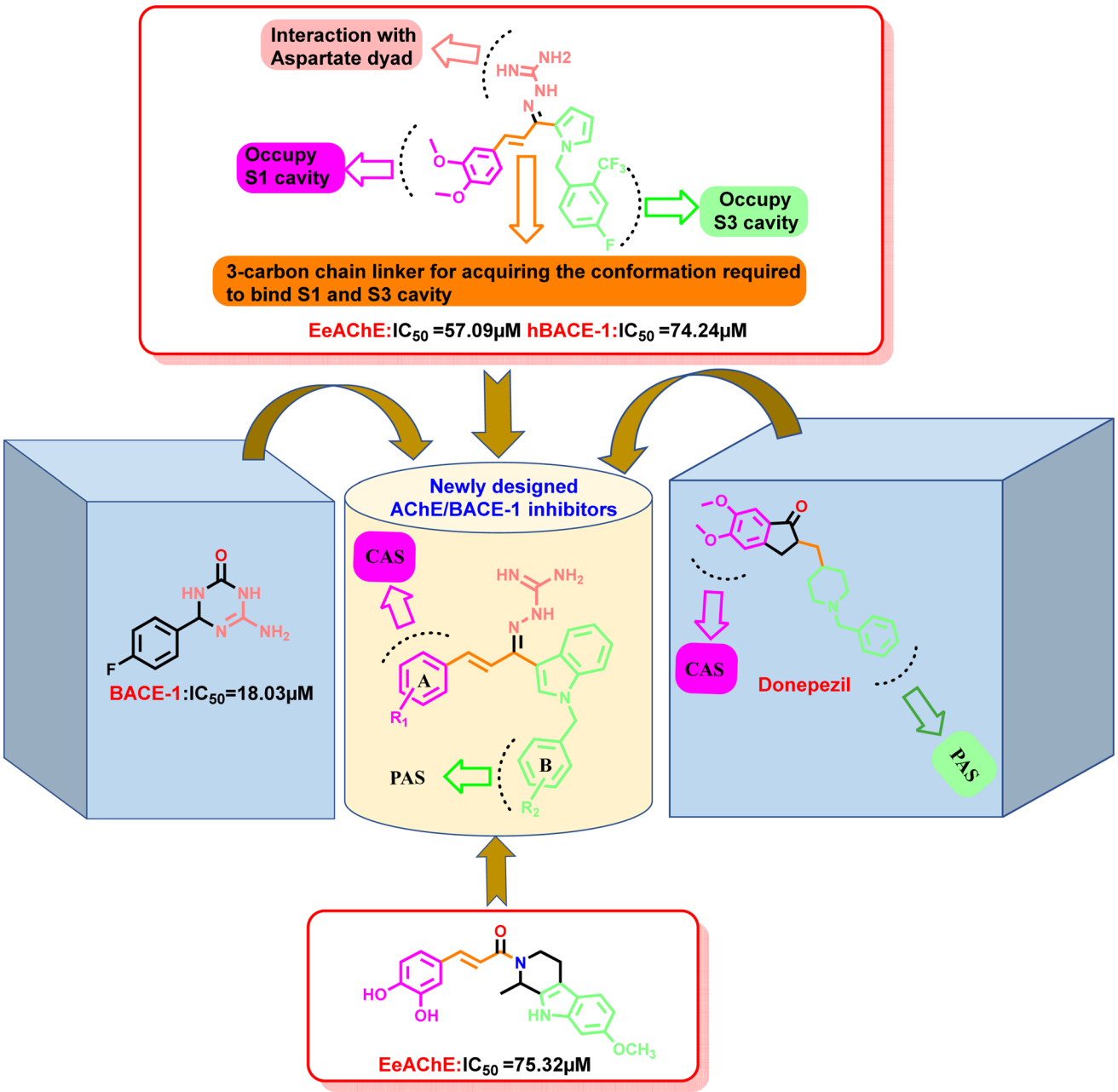

Fig. 2 Designing strategy for the development of indole-based dual inhibitors using molecular hybridization approach.

involvement of a histidine residue in the active site. The active site of AChE is a long and narrow gorge-like structure that spans about 20 Ångstroms in length. This pocket extends over halfway into the enzyme and gradually widens as it approaches the base. The gorge pocket contains only a few acidic amino acid residues; which includes Asp285, Glu273, Asp72 hydrogen bonded to Tyr334 and Glu199 respectively. For a compound to be considered an effective inhibitor of AChE, it is necessary for the inhibitor to engage with both the CAS amino acids – Trp86, Tyr337, Trp439, and Tyr341 – as well as the PAS amino acids – Trp286, Phe297, Phe295, Phe338, Tyr124, and Tyr72.

Insights into the key functional groups required to inhibit the activity of beta-secretase can be gleaned from the X-ray crystal structure of beta-secretase (PDB ID: 6UWP), which suggests that these groups must possess a basic nature. It is proposed that the presence of an H-bond donor group is essential for forming H-bonding interactions with the catalytic residues Asp-228 and Asp-32. Additionally, significant hydrophobic pockets (S1, S3, S2′) exist that are critical sites for beta-secretase inhibition and require hydrophobic groups to occupy these areas. The side chains of Tyr71, Phe108, Trp115, Ile118, and Leu30 collectively shape the S1 hydrophobic cleft. In a similar manner to S1, the S3 cavity is primarily hydrophobic and is formed by the side chains of Trp115 and Ile110, along with the main chains of Gln12, Gly11, Gly230, Thr231, Thr232,

and Ser35. Additionally, S2′ consists of the amino acid residues Ile126, Trp76, Val69, Arg128, and Tyr198.

Our previous results with allylidene hydrazinecarboximidamide derivatives showed that for optimal BACE 1 inhibition, a three-atom linker with aromatic groups on both ends to occupy the S1 and S3 cavities, as well as a hydrogen bond donor for binding to the aspartate dyad is essential.[24] Thus, *N*-benzylated indole on one end (ring B), substituted phenyl ring (ring A) on other end, and allylidene hydrazine scaffold on the linker was hypothesized.

2.2. Chemistry

The synthesis of all the final compounds **1a–s**, **2a–j**, **3a–l** were carried out as per the procedure detailed in Scheme 1. In the first step, *N*-benzyl indole was benzylated with substituted benzylbromides using potassium hydroxide in the presence of dimethylformamide (DMF). The Claisen–Schmidt condensation was followed by the addition of substituted benzaldehydes using sodium hydroxide in the presence of ethanol resulting the formation of chalcone derivatives. Further, chalcones undergo nucleophilic addition reaction using amino-guanidine hydrochloride in the presence of ethanol to provide the final compounds. The progress of the reactions was monitored by Thin Layer Chromatography (TLC) analysis (silica gel G_{60} F_{254}, Merck). ^{1}H and ^{13}C NMR spectra were recorded on a Bruker Avance II 400 spectrometer (400 MHz respectively) using DMSO-d_6 as solvent. HRMS-ESI^{+} mode analysis was performed on Agilent Technologies 6545, Version-Q-TOF B.06.01 (B6172 SP1).

2.3. AChE/BACE 1 inhibitory activity

The inhibitory activities of indol-3-yl-phenylallylidenehydrazinecarboximidamide hybrids **1a–s**, **2a–j**, **3a–l** against AChE and BACE 1 were evaluated by the Ellman technique and fluorescence resonance energy transfer (FRET) assay, respectively using donepezil and β-Secretase Inhibitor IV as reference standards. The results are shown in Tables 1–3.

Table 1 indicates the results for compounds **1a–s** of first series where ring A was substituted with electron withdrawing and donating substituents and ring B was unsubstituted. Overall, results validate the hypothesis that extension of our reported compound could result in pronounced dual inhibition of AChE and BACE 1. The compounds were active against both

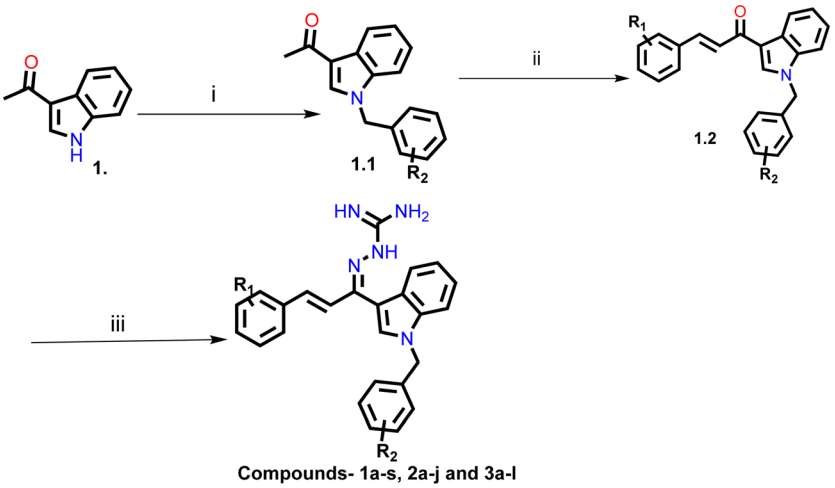

Compounds- 1a-s, 2a-j and 3a-l

1a, R_1=3,4-di-F, R_2=H
1b, R_1=4-tertbutyl, R_2=H
1c, R_1=3,4-di-OCH_3, R_2=H
1d, R_1=4-isopropyl, R_2=H
1e, R_1=3-OCH_3, R_2=H
1f, R_1=3-F, R_2=H
1g, R_1=4-dimethylamino,R_2=H
1h, R_1=3-Br, R_2=H
1i, R_1=4-Br, R_2=H
1j, R_1=2,5-di-OCH_3, R_2=H
1s, R_1=H, R_2=H
2c, R_1=H, R_2=3,5-di-CF_3
2d, R_1=H, R_2=2-CF_3,4-F
2e, R_1=H, R_2=2-CN
2f, R_1=H, R_2=4-Cl
2g, R_1=H, R_2=3,5-di-OCH_3
2h, R_1=H, R_2=2-F
2i, R_1=H, R_2=2-F,4-Br
2j, R_1=H, R_2=3-CN
1k, R_1=4-CH_3, R_2=H
1l, R_1=4-CN, R_2=H
1m, R_1=2,4-di-F, R_2=H
1n, R_1=2-NO_2, R_2=H
1o, R_1=3-Benzyloxy, R_2=H
1p, R_1=2,3-di-OCH_3, R_2=H
1q, R_1=4-Cl, R_2=H
1r, R_1=2-CH_3, R_2=H
2a, R_1=H, R_2=2,4-di-F
2b, R_1=H, R_2=4-CF_3

3a, R_1=4-CF_3, R_2=4-CF_3
3b, R_1=3,4-di-OCH_3, R_2=3,5-di-OCH_3
3c, R_1=4-tertbutyl, R_2=4-phenyl
3d, R_1=3,4-di-F, R_2=4-tertbutyl
3e, R_1=4-Benzyloxy, R_2=4-CH_3
3f, R_1=4-isopropyl, R_2=2,5-di-F
3g, R_1=4-tertbutyl, R_2=4-Br
3h, R_1=4-tertbutyl, R_2=4-tertbutyl
3i, R_1=4-Benzyloxy, R_2=3-Benzyloxy
3j, R_1=4-CF_3, R_2=4-butyl
3k, R_1=4-tertbutyl, R_2=4-CF_3
3l, R_1=2,5-di-OCH_3, R_2=4-butyl

Scheme 1 Reagents and conditions: (i) substituted benzyl bromide, KOH, DMF, ultra-sonication, 25 °C, 1 h (ii) substituted benzaldehyde, NaOH, EtOH, ultra-sonication, 25 °C, 30 min (iii) aminoguanidine-HCl, conc. HCl, EtOH, ultra-sonication, 25 °C, 2.0 h.

Table 1 Inhibitory activities of compounds **1a–s** on AChE and BACE 1[a]

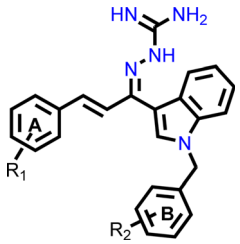

Compound	R_1	R_2	EeAChE IC_{50} (μM) ± SD	EeAChE PIC_{50} (μM)	hBACE 1 IC_{50} (μM) ± SD	hBACE 1 PIC_{50} (μM)
1a	3-4-di-F	H	77.24 ± 2.24	4.11	72.11 ± 0.01	4.14
1b	4-Tertbutyl	H	42.95 ± 0.48	4.37	97.36 ± 1.36	4.01
1c	3,4-di-OCH_3	H	77.08 ± 1.54	4.11	59.51 ± 0.21	4.23
1d	4-Isopropyl	H	146.25 ± 3.18	3.83	11.73 ± 0.15	4.93
1e	3-OCH_3	H	137.81 ± 0.14	3.86	117.24 ± 0.57	3.93
1f	3 F	H	67.01 ± 1.95	4.17	88.59 ± 0.32	4.05
1g	4-Dimethylamino	H	78.24 ± 2.28	4.11	89.02 ± 2.29	4.05
1h	3-Br	H	66.27 ± 1.72	4.18	15.10 ± 0.74	4.82
1i	4-Br	H	73.11 ± 2.07	4.14	97.83 ± 0.31	4.01
1j	2,5-di-OCH_3	H	60.96 ± 2.29	4.21	72.24 ± 1.76	4.14
1k	4-CH_3	H	185.50 ± 2.69	3.73	132.12 ± 0.28	3.88
1l	4-CN	H	60.93 ± 2.53	4.22	9.38 ± 0.50	5.03
1m	2,4-di-F	H	147.64 ± 3.11	3.83	12.81 ± 0.50	4.89
1n	2-NO_2	H	216.25 ± 3.61	3.67	12.35 ± 0.60	4.91
1o	3-Benzyloxy	H	126.61 ± 0.99	3.90	12.79 ± 0.42	4.89
1p	2,3-di-OCH_3	H	48.57 ± 1.51	4.31	134.25 ± 1.42	3.87
1q	4-Cl	H	82.64 ± 1.92	4.08	16.46 ± 0.39	4.78
1r	2-CH_3	H	46.78 ± 1.83	4.33	206.35 ± 3.75	3.69
1s	H	H	146.15 ± 0.07	3.84	202.75 ± 2.05	3.69
Donepezil			0.04 ± 0.01	7.40		
β-secretase inhibitor IV					0.02 ± 0.01	7.70

[a] Results are presented as mean ± SD, $n = 3$, eeAChE indicates AChE from electric eel and hBACE 1 indicates human BACE 1.

Table 2 Inhibitory activities of compounds **2a–j** on AChE and BACE 1[a]

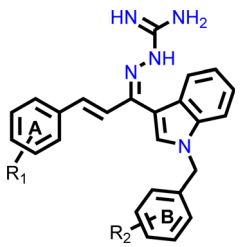

Compound	R_1	R_2	EeAChE IC_{50} (μM) ± SD	EeAChE PIC_{50} (μM)	hBACE 1 IC_{50} (μM) ± SD	hBACE 1 PIC_{50} (μM)
2a	H	2,4-di-F	46.44 ± 1.63	4.33	200.11 ± 1.98	3.70
2b	H	4-CF_3	55.99 ± 2.44	4.25	102.05 ± 1.06	3.99
2c	H	3,5-di-CF_3	56.58 ± 0.98	4.25	70.04 ± 0.87	4.15
2d	H	2-CF_3, 4 F	168.55 ± 1.91	3.77	140.85 ± 1.06	3.85
2e	H	2-CN	44.02 ± 0.19	4.36	196.75 ± 2.42	3.71
2f	H	4-Cl	42.78 ± 2.79	4.37	213.34 ± 2.26	3.67
2g	H	3,5-di-OCH_3	55.57 ± 0.72	4.26	83.43 ± 1.93	4.08
2h	H	2 F	62.86 ± 0.62	4.20	143.25 ± 0.21	3.84
2i	H	2 F, 4-Br	42.63 ± 1.58	4.37	185.95 ± 0.07	3.73
2j	H	3-CN	75.91 ± 0.32	4.12	178.25 ± 0.92	3.75
Donepezil			0.04 ± 0.01	7.40		
β-secretase inhibitor IV					0.02 ± 0.01	7.70

[a] Results are presented as mean ± SD, $n = 3$, eeAChE indicates AChE from electric eel and hBACE 1 indicates human BACE 1.

Table 3 Inhibitory activities of compounds **3a–l** on AChE and BACE 1[a]

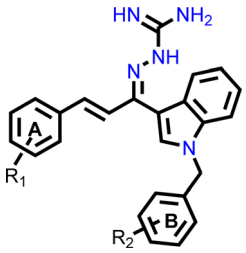

Compound	R_1	R_2	EeAChE IC_{50} (μM) ± SD	EeAChE PIC_{50} (μM)	hBACE 1 IC_{50} (μM) ± SD	hBACE 1 PIC_{50} (μM)
3a	4-CF_3	4-CF_3	38.41 ± 3.46	4.42	222.35 ± 0.49	3.65
3b	3,4-di-OCH_3	3,5-di-OCH_3	21.99 ± 0.65	4.66	197.55 ± 3.18	3.70
3c	4-Tertbutyl	4-Phenyl	16.58 ± 1.04	4.78	200.95 ± 3.82	3.70
3d	3,4-di-F	4-Tertbutyl	195.90 ± 1.73	3.71	76.87 ± 2.38	4.11
3e	4-Benzyloxy	4-CH_3	144.15 ± 1.77	3.84	107.15 ± 2.55	3.97
3f	4-Isopropyl	2,5-di-F	166.65 ± 2.12	3.78	82.15 ± 2.74	4.09
3g	4-Tertbutyl	4-Br	155.75 ± 2.62	3.81	178.25 ± 0.92	3.75
3h	4-Tertbutyl	4-Tertbutyl	55.66 ± 3.17	4.25	179.15 ± 0.78	3.75
3i	4-Benzyloxy	3-Benzyloxy	26.99 ± 0.13	4.57	189.05 ± 1.91	3.72
3j	4-CF_3	4-Butyl	13.38 ± 0.49	4.87	182.44 ± 1.41	3.74
3k	4-Tertbutyl	4-CF_3	207.13 ± 7.64	3.68	139.46 ± 1.98	3.86
3l	2,5-di-OCH_3	4-Butyl	58.44 ± 0.91	4.23	195.65 ± 3.04	3.71
Donepezil			0.04 ± 0.01	7.40		
β-secretase inhibitor IV					0.02 ± 0.01	7.70

[a] Results are presented as mean ± SD, $n = 3$, eeAChE indicates AChE from electric eel and hBACE 1 indicates human BACE 1.

enzymes however, with introduction of AChE inhibition, the BACE 1 inhibitory potential was decreased. It was found that electron donating substituents like 4-tertbutyl (**1b**) and 2-methyl (**1r**) on ring A, showed good AChE inhibition but decreased BACE 1 inhibitory activity. Conversely, substitution of electron withdrawing groups on ring A retained the BACE 1 inhibitory potential but affected the AChE inhibitory potency of compounds. It was also observed that the bulky substituent on ring A reduces the AChE inhibitory potential. Compound **1l**, which had *p*-cyano showed good AChE and BACE 1 inhibition activities and can be called the most active of the series.

In second series (compounds **2a–j**), ring B was substituted with various electron withdrawing and donating substituents while keeping ring A unsubstituted. It was observed that compared to ortho, para substitution of electron withdrawing groups on ring B was favorable for AChE inhibition. Compound **2c** showed comparable AChE and BACE 1 inhibition. Overall, it can be noted that the electron withdrawing substitution on ring B favors AChE inhibition. However, in general, substitute on ring B reduces BACE 1 inhibitory potential as shown in Table 2.

In previous two series, electron withdrawing group substitution on any of the ring favored AChE inhibition and substitution on ring B was unfavorable for BACE 1 inhibition. Also, substitution of bulky groups had impacted the activity. Therefore, in the third series (Table 3), both the rings (A and B) were substituted and in particular, the effect of bulky or electron withdrawing substituents was studied. It was expected that the substitution on both rings may potentiate the AChE inhibition and would also balance out the BACE 1 inhibition. However, substituting bulky or electron-withdrawing substituents on both rings resulted in significant improvement in AChE inhibition but compromised BACE 1 inhibition. This can be observed with compound **3j** which had bulky substituent on both rings and was the most potent AChE inhibitor of all compounds ($IC_{50} = 13.38$ μM).

2.4. Molecular modeling studies

2.4.1. Molecular docking analysis. To gain insights into the interactions between the synthesized compounds and the active site pocket of AChE and BACE 1, molecular docking studies were conducted. Docking was performed using Glide module of Schrödinger suite using crystal structure of human AChE and BACE 1 (PDB ID: 4EY7 and 6UWP, respectively). Validation studies were performed using co-crystallized ligands extracted from their respective crystal structures of proteins. Fig. 3 shows the validation results.

The analysis of compound **1l** in the active site of both the enzymes (Fig. 4), revealed the occupancy of substrate binding cavities and interactions with active site amino acids. It was seen that, along with occupancy of S1 cavity by ring A, ring B was accommodated in the S3 pocket of BACE 1. Its guanidinium moiety formed strong hydrogen bonding interactions with the key aspartate dyad Asp228 and Asp32. In case of AChE, ring A was seen to accommodate in the CAS pocket with enhanced π–π stacked interactions with Tyr341, Val294, Phe295 and ring B occupied PAS with π–π stacking with Trp86.

Compound **3j** having substituted ring A and substituted ring B, showed moderate BACE 1 inhibition and displayed hydrogen

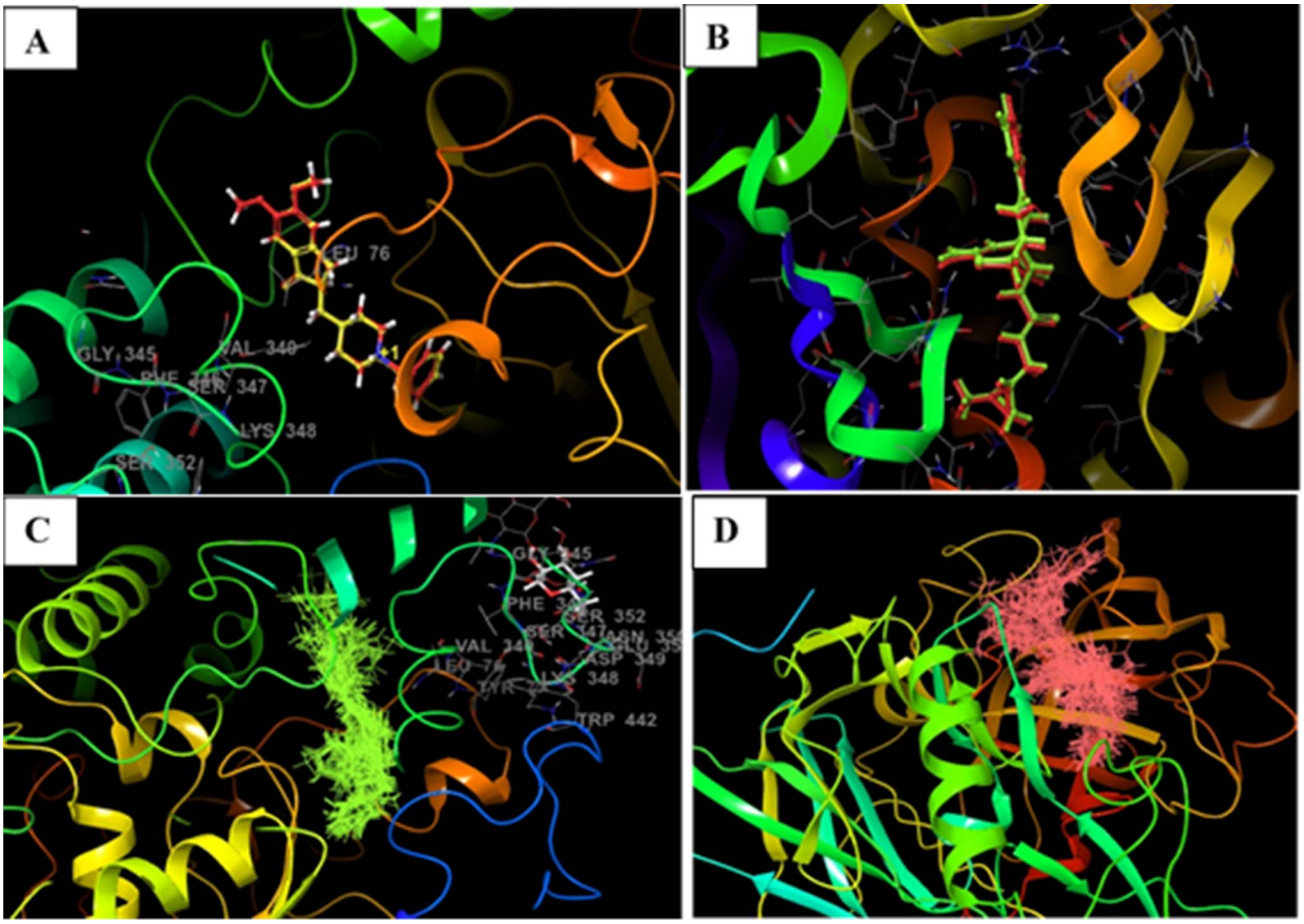

Fig. 3 Docking validation of 4EY7 and 6UWP (A) redocked pose of donepezil (red) superimposed with the co-crystallized ligand (yellow) (RMSD: 0.14 Å, Glide score:14.56); (B) redocked pose of QKA (red) superimposed with the co-crystallized ligand (green) (RMSD: 0.08 Å, Glide score:9.64); (C) and (D) show overlapping of all of the docked compounds within the active site of 4EY7 and 6UWP, respectively.

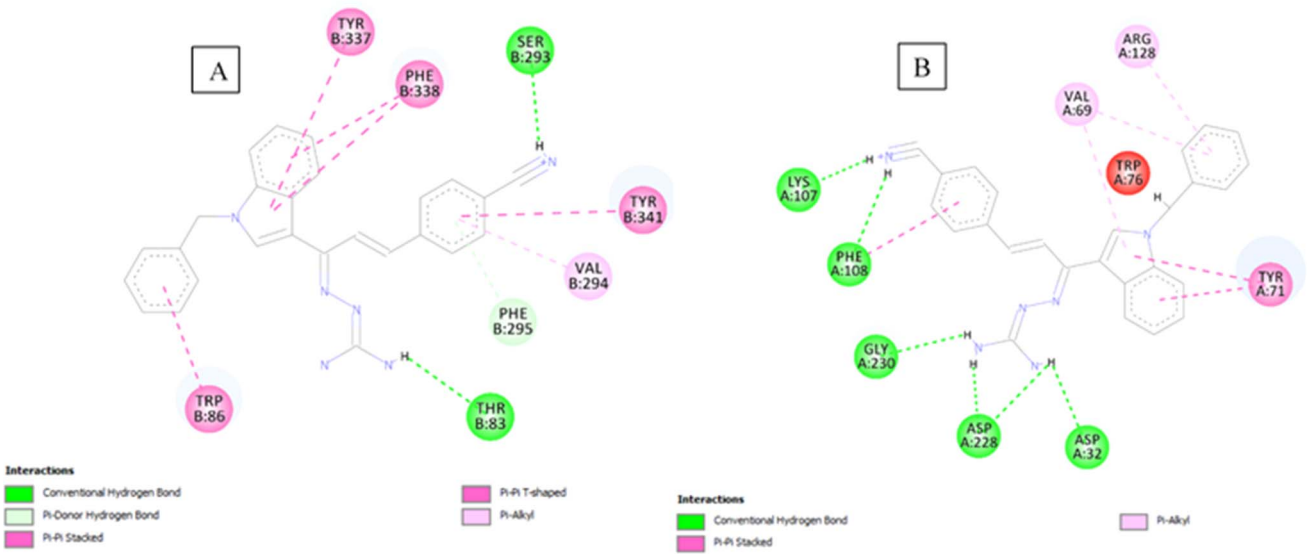

Fig. 4 (A) 2D interaction plot of **1l** in AChE (Glide score-11.08 kcal mol^{-1}); (B) 2D interaction plot of **1l** in BACE 1 (Glide score-10.98 kcal mol^{-1}).

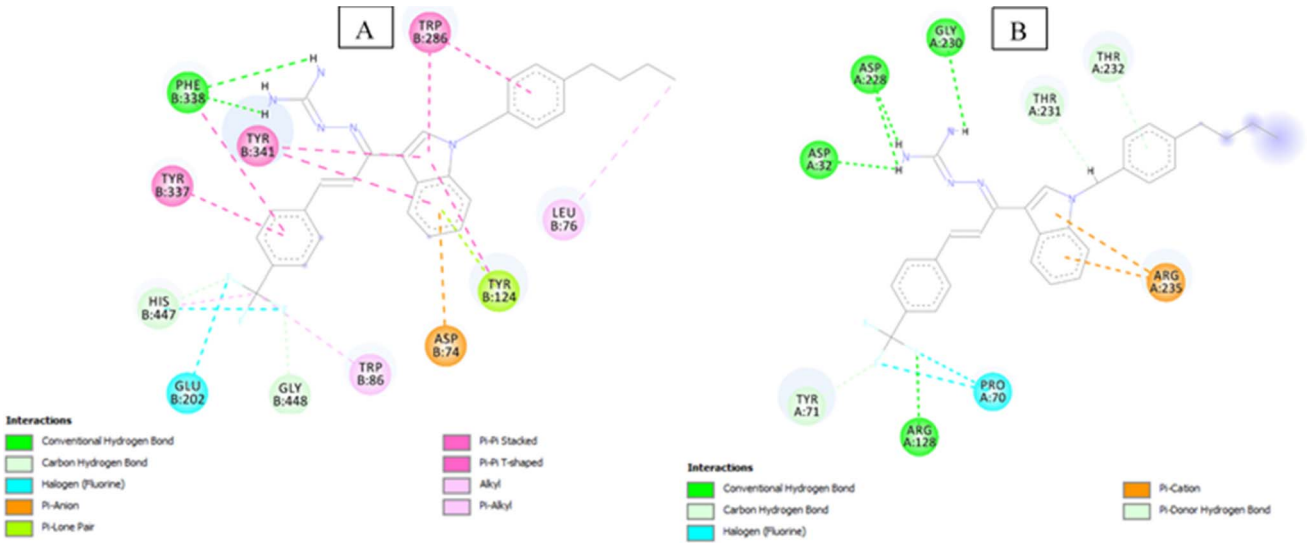

Fig. 5 (A) 2D interaction plot of **3j** in 4EY7 (Glide score-12.05 kcal mol^{-1}); (B) 2D interaction plot of **3j** in BACE 1 (Glide score-6.89 kcal mol^{-1}).

bonding interactions with aspartate dyad Asp228, Asp 32 and Gly230. It was seen ring A occupies the S1 cavity and ring B is oriented towards S3 cavity but the interactions are few. In case of AChE, **3j** was seen to accommodate the CAS pocket with enhanced π–π stacked interactions with Trp86, Gly448, Glu202, His447, hydrogen bonded with Phe338 and occupy PAS with π–π stacked with Tyr124, Trp286, Asp74, Leu76 were also observed and are shown in Fig. 5.

From the molecular docking studies, it was observed that substitution of ring A actually does not affect binding with BACE 1 active site but also makes the compound fit in active site of AChE. However, when the ring B is substituted, the substitution pushes the compound out of the binding pocket of BACE 1 and hence it does not show good BACE binding.

2.4.2. Molecular dynamics (MD) simulation. A molecular dynamics simulation study was conducted using the Desmond software developed by DE Shaw Research to analyze the stability of the binding between the compound **1l**-AChE/BACE 1 complex. The simulations took into account the flexibility of the protein environment and the behavior of water molecules in the vicinity. The root mean square deviations (RMSD) of the docked complexes were calculated and compared to the reference protein backbone structures, yielding values within a specific range. The simulation trajectories were further analyzed by examining the root mean square fluctuations (RMSF) values of compound **1l** within the AChE/BACE 1 complex. The results showed that the RMSF values remained relatively stable, indicating consistent trajectories for both the ligand and protein residues. Various methods, such as histograms, graphical representations, and time-line visualizations, were employed to comprehensively analyze the protein–ligand interaction. These analyses allowed the determination of the proportion of protein residues that interacted with compound **1l**. In the molecular dynamics studies of AChE, it was observed that compound **1l** exhibited significant interactions with PAS/CAS residues of AChE. Tyr341, a CAS residue, played a role in interacting with the indole scaffold of compound **1l** through π–π stacking (51% of the time) and charged interactions. Furthermore, Tyr124 and Trp286 residue in the PAS region exhibited a similar interaction to Trp341 residue, with a time-scale of 22% and 32% respectively. The aminoguanidinium nitrogen atom of compound **1l** formed hydrogen bonds with Tyr124 residue, with respective time-scale of 28%. Tyr72 formed a π-cation interaction with –NH functionality of **1l** (40%-time scale).

The molecular dynamics simulation of BACE 1 revealed that compound **1l** established strong and consistent interactions with the residues, namely Tyr71, Tyr198 and Arg235. The aminoguanidinium functionality of compound **1l** formed halogen bonding interaction with chlorine atom, accounting for 11% of the interactions observed throughout the simulation trajectories. Tyr198 formed a π–π stacked interaction with ring B and indole nucleus of **1l** with a time scale of 15% and 7%. Tyr71 residue engaged in a π–π stacked interaction with the ring A core of compound **1l**, representing 15% of the time-scale. Furthermore, Arg235 residue exhibited a π cation interaction with ring A core of **1l**, with a time scale of 5%. Overall, the results of the molecular dynamics simulation indicated that compound **1d** exhibited stable and well-balanced interactions within the active sites of both AChE and BACE 1 (Fig. 6 and 7).

The MM-GBSA (Molecular Mechanics Generalized Born and Surface Area) approach is used to determine the binding free energies of protein–ligand complexes. This method utilizes the VSGB 2.0 solvation model, which includes a variable-dielectric generalized Born model, and the OPLS3 force field with an implicit solvent model. The Prime MM-GBSA technique estimates the binding free energy based on these calculations.

$$\Delta G = E_{\text{complex}} - E_{\text{receptor}}\ (\text{from optimised complex}) - E_{\text{ligand}}\ (\text{from optimised complex})$$

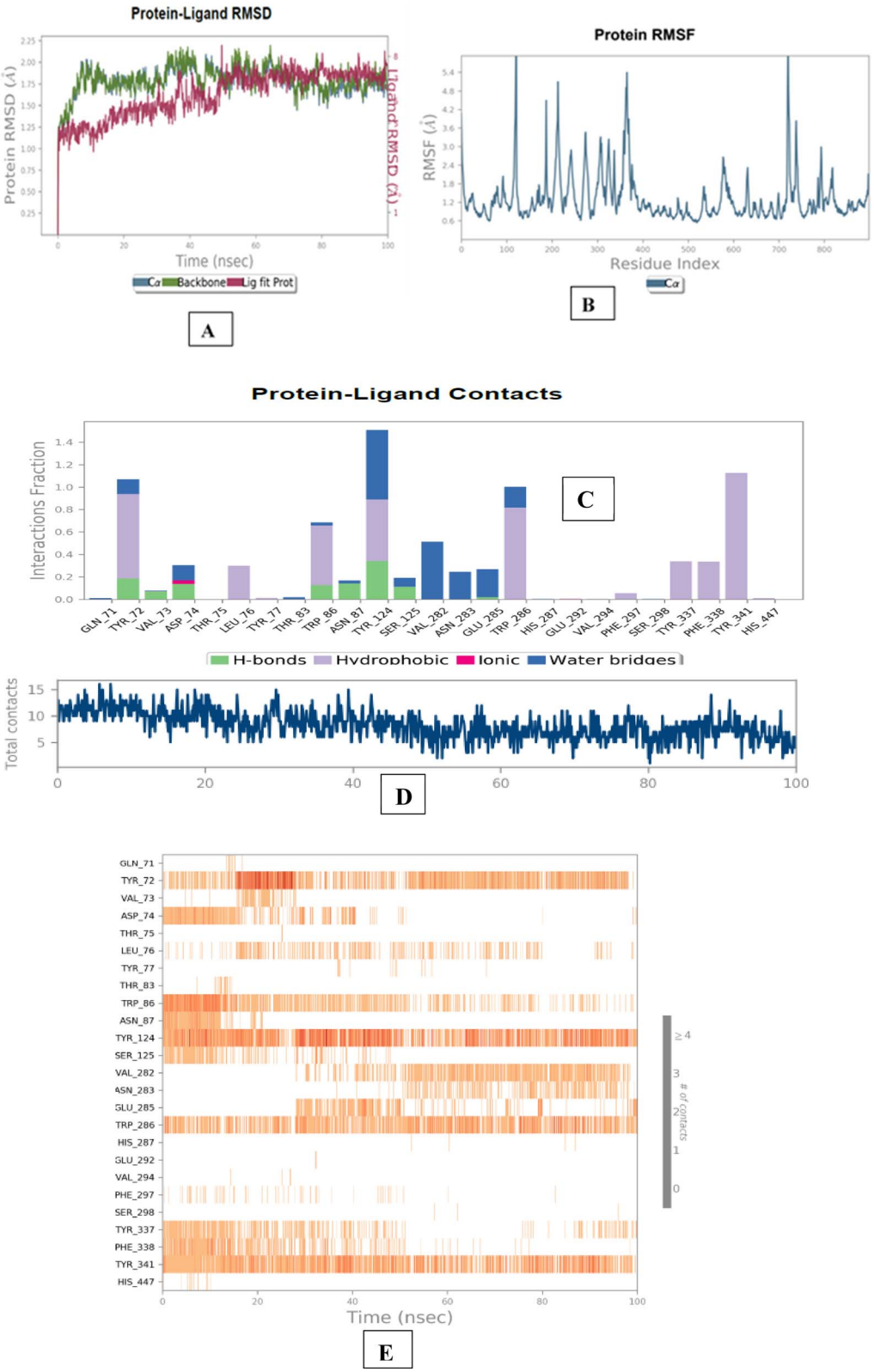

Fig. 6 Molecular dynamics studies of **1l**-AChE (4EY7) docked complex. [A] Comparative RMSD of AChE (protein backbone) and compound **1l** in the protein–ligand complex throughout the simulation period of 100 ns. [B] Graphical representation showing interactions with active site amino acid residues of PAS and CAS; [C] histogram showing interaction fractions with active amino acid residues; [D and E] timeline representation showing interaction with all the amino acid residues at each time frame.

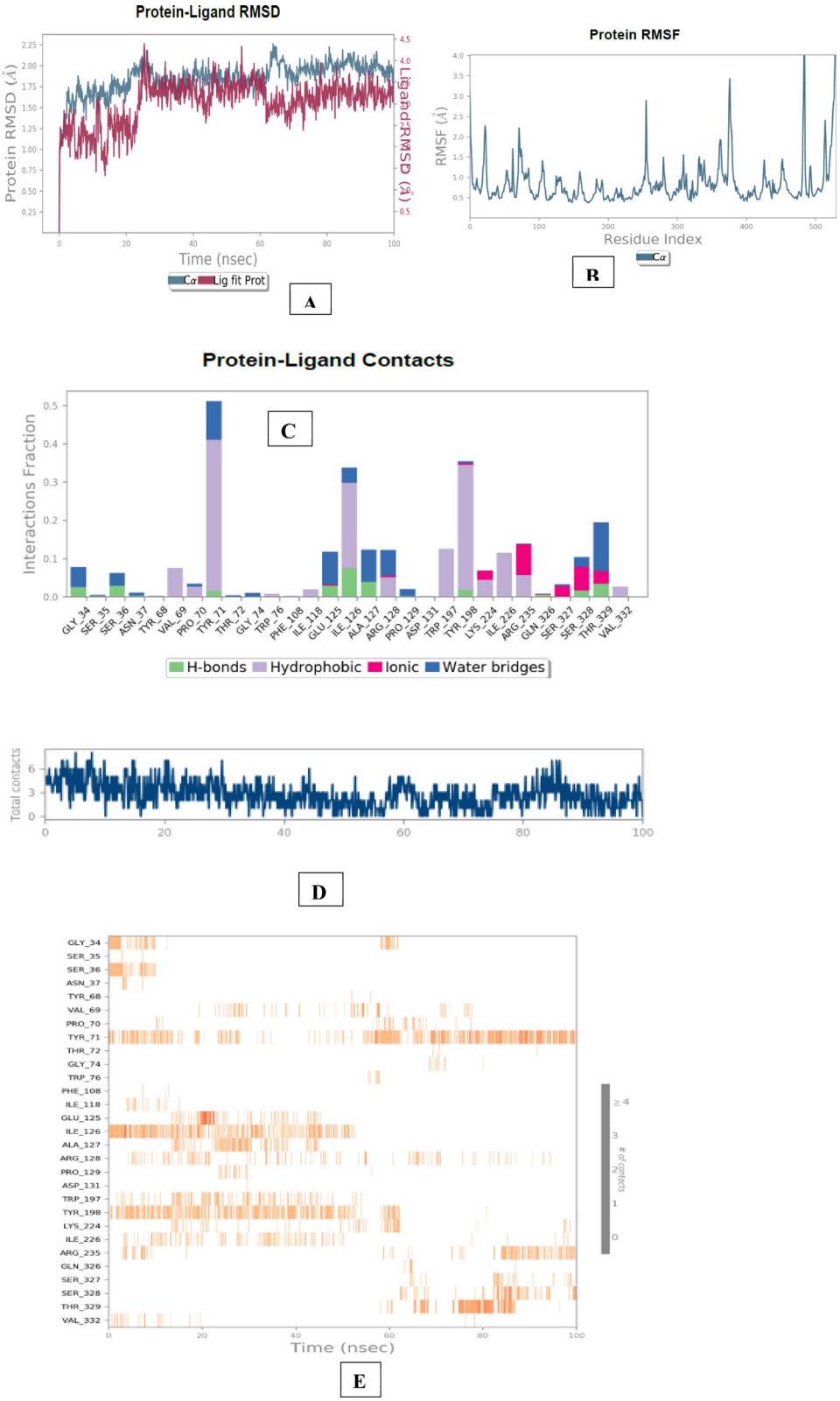

Fig. 7 Molecular dynamics studies of **1l**-BACE 1 (PDB ID: 6UWP) docked complex. [A] Comparative RMSD of BACE 1 (protein backbone) and compound **1l** in the protein–ligand complex throughout the simulation period of 100 ns. [B] Graphical representation showing interactions with active site amino acid residues (aspartate dyad); [C] histogram showing interaction fractions with active amino acid residues; [D and E] timeline representation showing interaction with all the amino acid residues at each time frame.

Table 4 The computed (MM-GBSA) binding free energies (ΔG bind) of the selected compounds against 4EY7 and 6UWP

Compound	MMGBSA score (4EY7) (kcal mol^{-1})	MMGBSA score (6UWP) (kcal mol^{-1})
1l	75.185 ± 5.692	71.401 ± 4.720

The analysis was performed by using the Prime module of Schrodinger with the help of thermal_MMGBSA.py script. The more negative MMGBSA score indicates the formation of more stable ligand-protein complexes. The score for the most active compound **1l** is given in Table 4.

2.5. Structure activity relationship

Based on the AChE and BACE 1 inhibitory activity of the compounds, a preliminary analysis of their structure–activity relationship was done. The potential of the compounds to inhibit AChE and BACE 1 varied with respect to the substitutions on the ring A and B respectively. In the case of molecular modeling studies of AChE, ring A occupies the CAS site of AChE, while the ring B is anchored to the PAS site. This binding pattern is mainly driven by hydrogen bonding and π–π stacking interactions, in which the aromatic ring B of the *N*-benzyl interacts with the Trp86 of PAS, ring A interacts with Trp286 of CAS, pyrrole interacts with residue Tyr337 Tyr341, Phe338 and guanidine interacts with the catalytic amino acid residues of AChE (Ser203, Glu202 and His447). Also, for BACE 1, it is observed that ring A occupies the S1 region, ring B is anchored to the S3 site and guanidine group can form H-bonding interactions with catalytic aspartate dyad that is, Asp32 and Asp228 respectively. When ring A alone was substituted with *p*-cyano group (compound **1l**), it was observed that compound **1l** had high docking score and maintained the BACE 1 inhibition as the parent compound[24] while also having AChE (IC_{50} value of 9.38 μM and 60.93 μM) inhibition. One possible explanation could be attributed to the robust interactions that were observed during the docking simulation: (i) ring B occupied S3 active site region with the indole scaffold π–π stacked to Tyr71 and Trp76; (ii) amino-guanidinium nitrogen formed hydrogen bonding interactions with catalytic aspartate dyad (Asp228 and Asp32). However, when ring B was substituted, all compounds in the series had weak BACE 1 inhibition indicating that the substituents on ring B is not favored for BACE 1 inhibition.

When both rings were substituted, again, BACE1 inhibition was not favored. The introduction of bulkier substituents on both rings such as compound **3j** showed pronounced AChE inhibition. This can be attributed to the strong hydrophobic interactions between the compound and the AChE binding site. However, increased IC_{50} values at BACE 1 indicating that bulkier substituents on both the rings was not favorable for BACE 1 inhibition (**3j**). When ring A was substituted with 4-tertbutyl and ring B with 4-phenyl (compound **3c**) showed pronounced AChE inhibition but compromised BACE 1 inhibition. As shown in Fig. 8, detailed SAR analysis of series **I**, **II** and **III** analogues were performed.

2.6. Theoretical prediction of the drug-likeness and ADME properties of representative target compounds by QikProp analysis

The drug-like characteristics of selected compounds were evaluated using Schrödinger's QikProp software, which indicated that its properties are comparable to that of donepezil (Table 5). Lipinski's rule of five includes mol MW (500), donor HB (0–6.0), acceptor HB (2.0–20) as well as the other important factors like SASA (300–1000), QPlogBB (−3.0 to 1.2), QPlogPo/w (−2.0 to 6.5), % human oral absorption (0 to 100% scale), QplogHERG (concern below −5) indicated that all the nominated compounds elicited "drug-like" properties.

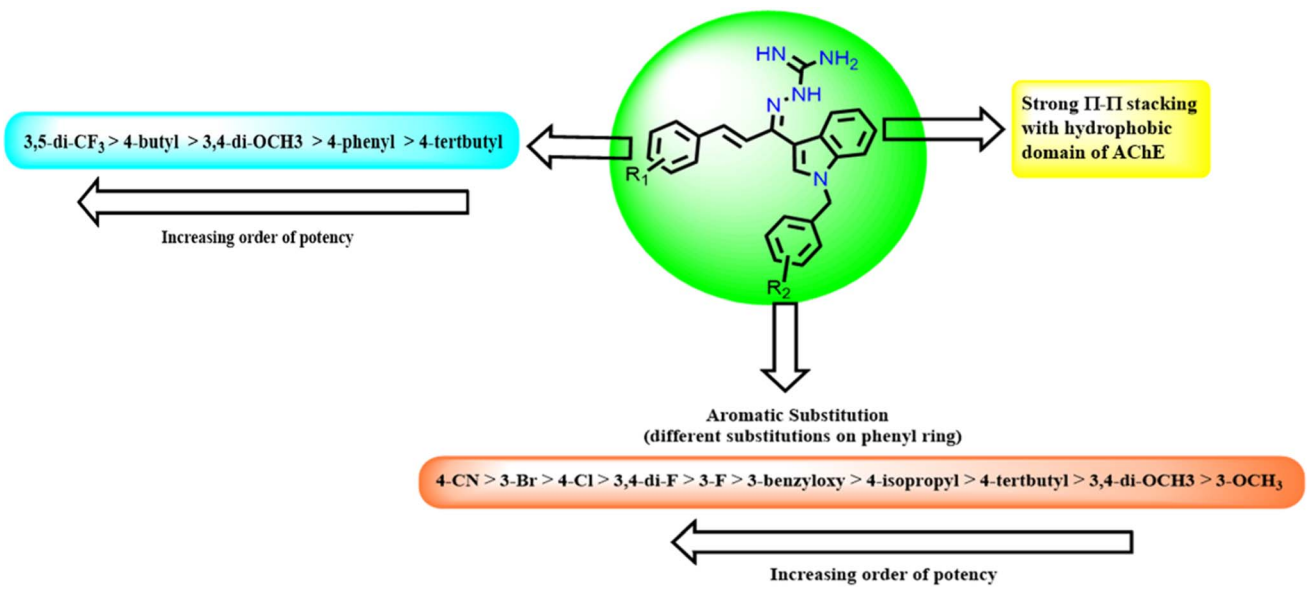

Fig. 8 Structure Activity Relationship (SAR) study of indol-3-yl-phenyl allylidene hydrazine carboximidamides analogues.

Table 5 Drug-likeness and ADME characteristics as determined by QikProp

Compound	[a]Mol_Wt	Donor HB[b]	Acceptor HB[c]	SASA[d]	QplogBB[e]	[f]Qplogo/w	% human oral absorption[g]	QplogHERG[h]
1a	429.47	4.0	3.5	728.37	−1.221	5.387	94.19%	−6.882
1b	449.59	4.0	3.0	830.21	−1.623	6.319	100.00%	−7.324
1c	453.54	4.0	5.0	772.82	−1.607	5.096	92.15%	−6.893
1d	435.57	4.0	3.5	806.50	−1.672	5.851	95.90%	−7.333
1f	411.48	4.0	3.5	704.62	−1.203	5.114	93.84%	−6.761
1g	436.55	4.0	4.5	768.24	−1.392	5.353	96.02%	−6.909
1h	472.38	4.0	3.5	731.53	−1.232	5.452	94.77%	−6.944
1j	453.54	4.0	5.0	761.45	−1.424	5.170	94.91%	−6.582
1l	418.50	4.0	4.5	762.67	−2.299	4.454	88.52%	−7.431
1m	429.47	4.0	3.5	683.42	−1.032	5.182	95.07%	−6.205
1n	438.48	4.0	4.5	721.14	−2.181	4.210	88.48%	−6.789
1o	499.61	4.0	4.2	836.10	−1.659	6.481	100.00%	−7.970
1q	427.93	4.0	3.0	749.32	−1.302	5.600	93.68%	−7.202
2c	529.48	4.0	3.5	781.18	−0.862	6.225	89.39%	−6.596
2g	453.54	4.0	5.0	744.25	−1.270	5.115	96.69%	−6.415
3b	513.59	4.0	6.5	794.22	−1.388	5.193	84.62%	−6.083
3c	525.69	4.0	3.0	918.59	−1.331	6.073	100.00%	−8.116
3i	605.73	4.0	5.0	996.50	−2.020	6.426	100.00%	−9.051
3j	517.59	4.0	3.5	850.32	−1.058	6.330	100.00%	−6.946
Donepezil	379.49	0.0	5.5	707.05	0.057	4.293	100.00%	−6.588

[a] Molecular weight of the compound. [b] Hydrogen bond donor in a molecule. [c] Hydrogen bond acceptor with in a molecule. [d] Total solvent accessible surface area in square angstroms using a probe with a 1.4 Å radius. [e] Predicted brain/blood partition coefficient. [f] Predicted octanol/water partition coefficient. [g] Predicted human oral absorption on 0 to 100% scale. [h] Predicted IC_{50} value for blockage of HERG K+ channels.

3. Conclusion

Herein, indol-3-yl-phenyl allylidene hydrazine carboximidamide derivatives have been identified as dual AChE/BACE 1 inhibitors. All the analogs showed dual inhibition and *in silico* binding with both the enzymes. It was observed that bulkier substitution favors AChE inhibition but reduces BACE 1 inhibitory potential. The compounds also showed excellent drug-likeness and ADME characteristics *in silico*. These *in vitro* results collectively warrant further investigation in suitable animal models for *in vivo* efficacy.

4. Experimental protocols

4.1. General procedures

All chemicals and reagents were purchased from commercial sources and used as such unless specifically mentioned. The advancement of the reactions was monitored and verified by means of thin-layer chromatography (TLC), using pre-coated TLC plates (E. Merck Kieselgel 60 F_{254}) embedded with a UV254 fluorescent indicator. Visualization of the components was achieved through exposure to ultraviolet light (at 254 nm) or other visualization agents like iodine vapors, potassium permanganate, *etc.* The purification of compounds was conducted on silica gel (230–400 mesh) with a solvent combination tailored for each individual experiment. Before utilization in chromatographic purification, all solvents were distilled. All final compounds were characterized by ^{1}H NMR, ^{13}C NMR spectroscopy using $CDCl_3$ or DMSO-D_6. ^{1}H NMR spectra were recorded on a Bruker Avance 400 MHz spectrometer Chemical shifts are given in parts per million (ppm), (δ relative to residual solvent peak for 1H). Data are reported as following: chemical shift, multiplicity (s = singlet, d = doublet, dd = doublet of doublets, t = triplet, q = quartet, m = multiplet, br = broad signal), and integration. HRMS-ESI$^+$ mode analysis was performed on Agilent Technologies 6545, Version-Q-TOF B.06.01(B6172 SP1) mass instrument.

4.1.1. General procedure for the synthesis of 1-(1-benzyl-1*H*-indol-3-yl)ethan-1-one (1.1). A round-bottom flask, with a volume of 100 mL, was utilized for containing 10 mL of DMF and 25.6 mmol of KOH. After being subjected to ultra-sonication for 15 minutes at room temperature, the mixture was supplemented with 8.5 mmol of 3-acetylindole, and stirring was sustained. Following a period of 30 minutes, a solution of substituted benzyl bromide (8.5 mmol) in 5 mL DMF was gradually drip-fed into the reaction mixture for a duration of 5 minutes. The reaction was then continued for 1 h. The ensuing mixture was then moved to ice-cold water and agitated for 5 minutes, which led to the emergence of a white precipitate. After filtration, the precipitate was retrieved and re-precipitated from ethanol to acquire 1-(1-benzyl-1*H*-indol-3-yl)ethan-1-one (**1.1**).

4.1.2. General procedure for the synthesis of (*E*)-1-(1-benzyl-1*H*-indol-3-yl)-3-phenylprop-2-en-1-one (1.2). A solution of an equimolar combination of substituted benzaldehyde (1 mmol) and compound **1.1** (1 mmol) was prepared in 15 mL of ethanol. Subsequently, the reaction mixture was subjected to continuous stirring, while a 10 mL solution of NaOH (6 g in 10 mL H_2O) was gradually dripped in. The reaction temperature was held within the range of 20–25 °C, utilizing a cold-water ultrasonic bath. TLC was utilized to monitor the course of the reaction. Following intense stirring for 20–25 minutes, the reaction mixture was removed from the ultrasonic water bath. The solid product was then precipitated by adding acidified cold water to neutralize the mixture. The crude product was

filtered, dried in the air, and then subjected to recrystallization using ethanol.

4.1.3. General procedure for the synthesis of (*Z*)-2-((*E*)-1-(1-benzyl-1*H*-indol-3-yl)-3-phenylallylidene)hydrazine-1-carboximidamide (1a–r, 2a–j and 3a–l). A mixture comprising of compound **1.2** (1 mmol) and aminoguanidine hydrochloride (0.11 g, 1 mmol) in equimolar amounts, was combined with 0.5 mL of HCl and 10 mL of EtOH. The resulting mixture was placed on an ultrasonic water bath for a duration of 2.0 hours. Reaction was monitored by TLC for completion. The TLC analysis was performed using a solvent system consisting of dichloromethane and methanol in varying ratios. After that, the solvent was evaporated under reduced pressure, and the residue was washed with water and then with diethyl ether. The final purification of the compounds was carried out through column chromatography.

4.1.4. (*Z*)-2-((*E*)-1-(1-Benzyl-1*H*-indol-3-yl)-3-(3,4-difluorophenyl)allylidene)hydrazine-1-carboximidamide (1a). Synthesized as per the general procedure described above. Yield 89%, yellow solid. ^{1}H NMR (400 MHz, DMSO-D$_6$) δ 11.12 (s, 1H), 10.10 (s, 1H), 9.55 (s, 1H), 8.33–8.02 (m, 2H), 7.64 (s, 4H), 7.49 (d, J = 7.9 Hz, 1H), 7.32 (dd, J = 10.1, 4.3 Hz, 2H), 7.28–7.21 (m, 3H), 7.20–7.10 (m, 2H), 5.47 (s, 2H), 2.41 (s, 2H), 1.90 (s, 1H); ^{13}C NMR (101 MHz, DMSO-D$_6$) δ 170.15, 159.61, 159.16, 156.42, 156.18, 151.71, 138.07, 137.37, 133.38, 129.08, 127.99, 127.71, 127.50, 127.33, 125.32, 123.63, 123.04, 121.46, 113.96, 110.94, 49.87, 25.19, 21.22, 18.56, 16.58; HRMS-ESI$^+$ calculated for $C_{25}H_{22}F_2N_5$ [M + H]$^+$ 430.1843, found: 430.1839.

4.1.5. (*Z*)-2-((*E*)-1-(1-Benzyl-1*H*-indol-3-yl)-3-(4-(*tert*-butyl)phenyl)allylidene)hydrazine-1-carboximidamide (1b). Synthesized as per the general procedure described above. Yield 92%, white solid. ^{1}H NMR (400 MHz, DMSO-D$_6$) δ 11.12 (s, 1H), 10.11 (s, 1H), 9.56 (s, 1H), 8.33–8.02 (m, 2H), 7.96–7.54 (m, 6H), 7.51–7.45 (m, 1H), 7.37–7.29 (m, 2H), 7.28–7.19 (m, 3H), 7.18–7.11 (m, 1H), 5.52–5.45 (m, 2H), 3.42 (s, 9H), 2.41 (s, 2H), 1.90 (s, 1H); ^{13}C NMR (101 MHz, DMSO-D$_6$) δ 170.16, 160.34, 159.59, 159.14, 156.22, 151.71, 138.05, 137.35, 133.37, 129.06, 128.19, 127.98, 127.76, 127.69, 127.49, 125.27, 123.62, 123.03, 121.54, 121.45, 113.92, 110.93, 60.23, 49.86, 31.53, 21.21, 18.59, 16.58, 14.42; HRMS-ESI$^+$ calculated for $C_{29}H_{31}N_5$ [M + H]$^+$ 450.2649, found: 450.2646.

4.1.6. (*Z*)-2-((*E*)-1-(1-Benzyl-1*H*-indol-3-yl)-3-(3,4-dimethoxyphenyl)allylidene)hydrazine-1-carboximidamide (1c). Synthesized as per the general procedure described above. Yield 85%, yellow solid. ^{1}H NMR (400 MHz, DMSO-D$_6$) δ 11.12 (s, 1H), 8.45–8.04 (m, 2H), 7.98–7.56 (m, 4H), 7.56–7.38 (m, 2H), 7.38–7.28 (m, 3H), 7.28–7.22 (m, 3H), 7.22–7.10 (m, 2H), 5.49 (d, J = 17.4 Hz, 2H), 4.06–3.28 (m, 6H), 2.42 (s, 2H), 2.00–1.87 (m, 1H); ^{13}C NMR (101 MHz, DMSO-D$_6$) δ 170.16, 159.16, 156.23, 155.37, 151.72, 138.07, 137.37, 133.38, 129.28, 129.08, 127.99, 127.73, 127.50, 127.35, 125.36, 125.29, 123.64, 123.04, 121.46, 113.95, 111.79, 110.94, 49.87, 25.19, 21.22, 16.56, 14.80; HRMS-ESI$^+$ calculated for $C_{27}H_{28}N_5O_2$ [M + H]$^+$ 454.2239, found: 454.2236.

4.1.7. (*Z*)-2-((*E*)-1-(1-Benzyl-1*H*-indol-3-yl)-3-(4-isopropylphenyl)allylidene)hydrazine-1-carboximidamide (1d). Synthesized as per the general procedure described above. Yield 88%, brown solid. ^{1}H NMR (400 MHz, DMSO-D$_6$) δ 11.07 (d, J = 46.9 Hz, 1H), 10.11 (s, 1H), 8.39–8.16 (m, 1H), 8.01–7.58 (m, 5H), 7.55–7.39 (m, 3H), 7.32 (ddd, J = 11.2, 9.9, 4.9 Hz, 3H), 7.28–7.23 (m, 2H), 7.15 (dddd, J = 22.7, 17.4, 7.5, 4.6 Hz, 3H), 5.66–5.31 (m, 2H), 3.40 (s, 6H), 2.42 (s, 2H), 1.91 (d, J = 6.8 Hz, 1H); ^{13}C NMR (101 MHz, DMSO-D$_6$) δ 170.15, 159.60, 159.15, 158.83, 156.40, 156.22, 155.18, 151.70, 138.06, 137.36, 133.37, 129.06, 127.97, 127.68, 127.49, 127.10, 125.28, 123.63, 123.03, 121.45, 113.93, 110.93, 49.87, 25.14, 24.20, 21.22, 18.59, 16.58; HRMS-ESI$^+$ calculated for $C_{28}H_{30}N_5$ [M + H]$^+$ 436.2501, found: 436.2500.

4.1.8. (*Z*)-2-((*E*)-1-(1-Benzyl-1*H*-indol-3-yl)-3-(3-methoxyphenyl)allylidene)hydrazine-1-carboximidamide (1e). Synthesized as per the general procedure described above. Yield 91%, brown solid. ^{1}H NMR (400 MHz, DMSO-D$_6$) δ 11.61 (d, J = 78.1 Hz, 1H), 10.08 (t, J = 11.1 Hz, 1H), 8.33–7.82 (m, 2H), 7.79–7.47 (m, 4H), 7.43–7.37 (m, 1H), 7.35–7.23 (m, 4H), 7.22–7.11 (m, 2H), 6.96 (ddd, J = 22.2, 17.5, 7.4 Hz, 2H), 6.82–6.61 (m, 1H), 5.43 (ddd, J = 73.2, 44.1, 32.3 Hz, 2H), 4.00–3.53 (m, 3H), 2.38 (d, J = 32.1 Hz, 1H), 2.03–1.79 (m, 1H); ^{13}C NMR (101 MHz, DMSO-D$_6$) δ 170.16, 160.08, 156.20, 140.82, 138.16, 133.36, 131.83, 130.20, 129.12, 129.08, 129.03, 128.09, 128.00, 127.99, 127.73, 127.69, 127.50, 127.45, 122.94, 120.10, 56.00, 55.59, 49.84, 25.18, 21.29, 16.82; HRMS-ESI$^+$ calculated for $C_{26}H_{26}N_5O$[M + H]$^+$ 424.2137, found: 424.2140.

4.1.9. (*Z*)-2-((*E*)-1-(1-Benzyl-1*H*-indol-3-yl)-3-(3-fluorophenyl)allylidene)hydrazine-1-carboximidamide (1f). Synthesized as per the general procedure described above. Yield 85%, yellow solid. ^{1}H NMR (400 MHz, DMSO-D$_6$) δ 11.08 (s, 1H), 8.39–7.91 (m, 2H), 7.67 (dd, J = 34.7, 26.0 Hz, 4H), 7.56–7.36 (m, 3H), 7.36–7.29 (m, 2H), 7.29–7.23 (m, 3H), 7.16 (ddd, J = 24.8, 15.9, 8.7 Hz, 3H), 5.72–5.19 (m, 2H), 2.41 (s, 2H), 2.01–1.85 (m, 1H); ^{13}C NMR (101 MHz, DMSO-D$_6$) δ 170.15, 159.11, 156.36, 156.29, 156.17, 151.74, 138.06, 137.36, 133.37, 129.07, 129.01, 127.98, 127.69, 127.48, 127.37, 125.28, 123.62, 123.04, 121.45, 113.93, 110.94, 49.87, 25.15, 21.22, 16.53; HRMS-ESI$^+$ calculated for $C_{25}H_{23}FN_5$ [M + H]$^+$ 412.1937, found: 412.1933.

4.1.10. (*Z*)-2-((*E*)-1-(1-Benzyl-1*H*-indol-3-yl)-3-(4-(dimethylamino)phenyl)allylidene)hydrazine-1-carboximidamide (1g). Synthesized as per the general procedure described above. Yield 84%, cream white solid. ^{1}H NMR (400 MHz, DMSO-D$_6$) δ 11.08 (s, 1H), 8.24 (dd, J = 36.9, 16.6 Hz, 2H), 7.72–7.55 (m, 3H), 7.50 (t, J = 8.9 Hz, 1H), 7.39–7.30 (m, 3H), 7.29–7.23 (m, 4H), 7.22–7.12 (m, 2H), 7.05 (t, J = 11.6 Hz, 1H), 6.73 (dd, J = 19.9, 10.4 Hz, 1H), 5.47 (s, 2H), 3.50–3.24 (m, 6H), 2.85 (s, 1H), 2.42 (s, 2H); ^{13}C NMR (101 MHz, DMSO-D$_6$) δ 156.18, 151.74, 138.05, 137.72, 137.36, 133.38, 129.12, 129.07, 128.10, 127.98, 127.68, 127.49, 126.62, 125.28, 123.63, 123.04, 121.80, 121.46, 113.93, 113.00, 111.27, 110.94, 107.45, 58.99, 49.87, 45.19, 16.54; HRMS-ESI$^+$ calculated for $C_{27}H_{29}N_6$ [M + H]$^+$ 437.2454, found: 437.2462.

4.1.11. (*Z*)-2-((*E*)-1-(1-Benzyl-1*H*-indol-3-yl)-3-(3-bromophenyl)allylidene)hydrazine-1-carboximidamide (1h). Synthesized as per the general procedure described above. Yield 93%, yellow solid. ^{1}H NMR (400 MHz, DMSO-D$_6$) δ 11.13 (s, 1H), 8.35–7.83 (m, 3H), 7.83–7.54 (m, 4H), 7.54–7.36 (m, 2H), 7.36–7.29 (m, 2H), 7.28–7.22 (m, 3H), 7.22–6.88 (m, 3H), 5.63–5.34 (m, 2H), 2.42 (s, 2H), 2.00–1.88 (m, 1H); ^{13}C NMR (101 MHz,

DMSO-D_6) δ 170.15, 159.14, 156.21, 151.71, 138.06, 137.36, 133.36, 131.17, 129.07, 127.98, 127.65, 127.49, 127.38, 125.29, 123.63, 123.04, 121.45, 113.95, 110.94, 49.87, 25.15, 21.22, 18.57, 16.56, 14.56; HRMS-ESI$^+$ calculated for $C_{25}H_{23}BrN_5$ [M + H]$^+$ 472.1137, found: 472.1131.

4.1.12. (*Z*)-2-((*E*)-1-(1-Benzyl-1*H*-indol-3-yl)-3-(4-bromophenyl)allylidene)hydrazine-1-carboximidamide (1i). Synthesized as per the general procedure described above. Yield 78%, yellow creamish solid. ^{1}H NMR (400 MHz, DMSO-D_6) δ 11.12 (s, 1H), 8.36–7.99 (m, 2H), 7.75 (ddd, J = 39.0, 23.9, 6.0 Hz, 4H), 7.59–7.37 (m, 3H), 7.36–7.29 (m, 2H), 7.25 (dd, J = 7.2, 3.9 Hz, 3H), 7.22–6.88 (m, 3H), 5.49 (d, J = 14.4 Hz, 2H), 2.42 (s, 2H), 2.01–1.84 (m, 1H); ^{13}C NMR (101 MHz, DMSO-D_6) δ 170.15, 159.13, 156.21, 151.71, 138.06, 137.36, 133.36, 129.07, 127.98, 127.75, 127.66, 127.48, 127.44, 125.29, 123.62, 123.03, 121.45, 113.95, 110.93, 60.19, 49.87, 25.15, 21.22, 18.51, 16.55; HRMS-ESI$^+$ calculated for $C_{25}H_{23}BrN_5$ [M + H]$^+$ 472.1137, found: 472.1144.

4.1.13. (*Z*)-2-((*E*)-1-(1-Benzyl-1*H*-indol-3-yl)-3-(2,5-dimethoxyphenyl)allylidene)hydrazine-1-carboximidamide (1j). Synthesized as per the general procedure described above. Yield 93%, yellow solid. ^{1}H NMR (400 MHz, DMSO-D_6) δ 11.11 (s, 1H), 8.32–8.02 (m, 2H), 8.01–7.60 (m, 4H), 7.58–7.37 (m, 2H), 7.36–7.28 (m, 2H), 7.28–7.23 (m, 3H), 7.23–7.06 (m, 2H), 7.06–6.77 (m, 1H), 5.49 (d, J = 15.1 Hz, 2H), 3.85–3.37 (m, 6H), 2.42 (s, 2H), 2.06–1.82 (m, 1H); ^{13}C NMR (101 MHz, DMSO-D_6) δ 159.14, 156.21, 151.72, 138.05, 137.36, 133.38, 129.06, 127.98, 127.64, 127.49, 127.27, 125.28, 125.09, 123.63, 123.04, 121.45, 113.93, 113.45, 111.95, 111.80, 110.94, 56.69, 56.43, 49.87, 21.57, 21.22, 16.57; HRMS-ESI$^+$ calculated for $C_{27}H_{28}N_5O_2$ [M + H]$^+$ 454.2249, found: 454.2254.

4.1.14. (*Z*)-2-((*E*)-1-(1-Benzyl-1*H*-indol-3-yl)-3-(*p*-tolyl) allylidene)hydrazine-1-carboximidamide (1k). Synthesized as per the general procedure described above. Yield 83%, white solid. ^{1}H NMR (400 MHz, DMSO-D_6) δ 11.08 (d, J = 49.5 Hz, 1H), 10.10 (d, J = 7.5 Hz, 1H), 9.55 (s, 1H), 8.92–8.68 (m, 1H), 8.36–8.13 (m, 1H), 8.01–7.78 (m, 2H), 7.71–7.63 (m, 2H), 7.59–7.46 (m, 2H), 7.43–7.28 (m, 4H), 7.27–7.21 (m, 2H), 7.20–7.07 (m, 3H), 5.60–5.28 (m, 2H), 2.43–2.28 (m, 2H), 1.98–1.89 (m, 1H); ^{13}C NMR (101 MHz, DMSO-D_6) δ 170.14, 159.66, 159.16, 156.24, 155.07, 151.76, 138.06, 137.33, 136.97, 133.44, 129.75, 129.06, 128.61, 127.96, 127.71, 127.68, 127.49, 125.28, 121.45, 113.93, 111.69, 49.87, 25.14, 21.22, 18.61, 16.60; HRMS-ESI$^+$ calculated for $C_{26}H_{26}N_5$ [M + H]$^+$ 408.2182, found: 408.2179.

4.1.15. (*Z*)-2-((*E*)-1-(1-Benzyl-1*H*-indol-3-yl)-3-(4-cyanophenyl)allylidene)hydrazine-1-carboximidamide (1l). Synthesized as per the general procedure described above. Yield 82%, yellow solid. ^{1}H NMR (400 MHz, DMSO-D_6) δ 11.08 (d, J = 49.5 Hz, 1H), 10.25–10.02 (m, 1H), 9.55 (s, 1H), 8.31–7.86 (m, 2H), 7.84–7.41 (m, 6H), 7.38–7.18 (m, 6H), 7.15–6.97 (m, 1H), 5.49 (dt, J = 64.8, 28.7 Hz, 2H), 2.42 (s, 1H), 1.99–1.89 (m, 1H); ^{13}C NMR (101 MHz, DMSO-D_6) δ 170.14, 159.17, 156.24, 151.69, 138.06, 137.36, 133.38, 129.14, 129.12, 129.07, 129.00, 128.69, 128.30, 127.98, 127.73, 127.67, 127.49, 125.33, 123.64, 123.03, 121.45, 113.94, 110.79, 49.87, 21.23, 16.60; HRMS-ESI$^-$ calculated for $C_{26}H_{21}N_6$ [M − H]$^+$ 417.0698, found: 417.0694.

4.1.16. (*Z*)-2-((*E*)-1-(1-Benzyl-1*H*-indol-3-yl)-3-(2,4-difluorophenyl)allylidene)hydrazine-1-carboximidamide (1m). Synthesized as per the general procedure described above. Yield 81%, yellow solid. ^{1}H NMR (400 MHz, DMSO-D_6) δ 10.19–10.05 (m, 1H), 9.54 (s, 1H), 8.31–7.94 (m, 2H), 7.61 (dddd, J = 25.8, 22.1, 20.3, 16.0 Hz, 6H), 7.39–7.20 (m, 5H), 7.19–6.98 (m, 2H), 6.95–6.50 (m, 1H), 5.60–5.34 (m, 2H), 2.42 (s, 1H), 1.91 (d, J = 6.8 Hz, 1H); ^{13}C NMR (101 MHz, DMSO-D_6) δ 170.11, 159.61, 159.16, 156.24, 138.09, 136.97, 133.43, 131.86, 129.08, 129.04, 129.01, 127.97, 127.82, 127.67, 127.49, 127.46, 125.29, 122.95, 121.22, 111.54, 49.82, 25.12, 21.22, 18.60, 16.59; HRMS-ESI$^+$ calculated for $C_{25}H_{22}$ F_2N_5 [M + H]$^+$ 430.1740, found: 430.1736.

4.1.17. (*Z*)-2-((*E*)-1-(1-Benzyl-1*H*-indol-3-yl)-3-(2-nitrophenyl)allylidene)hydrazine-1-carboximidamide (1n). Synthesized as per the general procedure described above. Yield 89%, brown solid. ^{1}H NMR (400 MHz, DMSO-D_6) δ 11.08 (d, J = 50.3 Hz, 1H), 10.08 (d, J = 33.9 Hz, 1H), 9.55 (s, 1H), 8.36–7.85 (m, 2H), 7.59 (d, J = 43.4 Hz, 5H), 7.52–7.39 (m, 2H), 7.36–7.29 (m, 2H), 7.28–7.22 (m, 2H), 7.22–6.99 (m, 2H), 5.47 (s, 2H), 1.96–1.89 (m, 2H); ^{13}C NMR (101 MHz, DMSO-D_6) δ 170.15, 160.04, 159.17, 156.43, 156.35, 156.24, 155.12, 151.70, 138.05, 137.35, 133.38, 129.06, 127.97, 127.49, 125.28, 123.63, 123.03, 121.45, 113.92, 110.93, 49.87, 25.13, 21.23, 18.61, 16.60; HRMS-ESI$^+$ calculated for $C_{25}H_{22}N_6O_2$ [M + H]$^+$ 438.1780, found: 438.1776.

4.1.18. (*Z*)-2-((*E*)-1-(1-Benzyl-1*H*-indol-3-yl)-3-(3-(benzyloxy) phenyl)allylidene)hydrazine-1-carboximidamide (1o). Synthesized as per the general procedure described above. Yield 95%, yellow solid. ^{1}H NMR (400 MHz, DMSO-D_6) δ 11.16 (s, 1H), 10.10 (d, J = 31.6 Hz, 1H), 9.43 (d, J = 110.8 Hz, 1H), 8.36–8.08 (m, 3H), 7.87 (dd, J = 96.5, 9.5 Hz, 3H), 7.67 (s, 3H), 7.50 (dd, J = 16.5, 6.6 Hz, 2H), 7.38 (d, J = 5.5 Hz, 1H), 7.37–7.33 (m, 1H), 7.30 (d, J = 6.5 Hz, 2H), 7.25 (d, J = 6.3 Hz, 4H), 7.20 (d, J = 7.0 Hz, 1H), 7.17 (d, J = 3.2 Hz, 1H), 7.16–7.05 (m, 1H), 5.57–5.34 (m, 2H), 1.97–1.88 (m, 2H); ^{13}C NMR (101 MHz, DMSO-D_6) δ 170.16, 159.62, 159.19, 156.44, 156.26, 155.11, 151.70, 138.05, 137.35, 133.38, 129.06, 128.87, 128.82, 128.28, 128.15, 127.97, 127.69, 127.49, 127.40, 125.28, 123.63, 123.03, 121.46, 113.93, 110.93, 56.49, 49.87, 25.13, 21.23, 19.03, 18.62, 16.62; HRMS-ESI$^+$ calculated for $C_{32}H_{30}N_5O$ [M + H]$^+$ 500.2337, found: 500.2335.

4.1.19. (*Z*)-2-((*E*)-1-(1-Benzyl-1*H*-indol-3-yl)-3-(2,3-dimethoxyphenyl)allylidene)hydrazine-1-carboximidamide (1p). Synthesized as per the general procedure described above. Yield 79%, light yellow solid. ^{1}H NMR (400 MHz, DMSO-D_6) δ 11.71–10.98 (m, 1H), 8.92–7.90 (m, 2H), 7.89–7.44 (m, 5H), 7.43–7.24 (m, 5H), 7.23–7.08 (m, 3H), 7.06–6.70 (m, 1H), 5.74–5.19 (m, 2H), 3.89–3.34 (m, 6H), 2.42 (s, 1H), 2.01–1.87 (m, 1H); ^{13}C NMR (101 MHz, DMSO-D_6) δ 159.62, 156.25, 153.08, 147.68, 138.15, 138.06, 133.39, 129.68, 129.07, 129.03, 127.98, 127.67, 127.58, 127.49, 127.40, 125.29, 123.04, 121.46, 113.93, 61.23, 60.68, 56.25, 50.03, 49.10, 25.13, 18.61, 16.60; HRMS-ESI$^+$ calculated for $C_{27}H_{28}N_5O_2$ [M + H]$^+$ 454.2208, found: 454.2204.

4.1.20. (*Z*)-2-((*E*)-1-(1-Benzyl-1*H*-indol-3-yl)-3-(4-chlorophenyl)allylidene)hydrazine-1-carboximidamide (1q). Synthesized as per the general procedure described above. Yield 79%, light brown solid. ^{1}H NMR (400 MHz, DMSO-D_6) δ 8.39–7.97 (m, 2H), 7.95–7.69 (m, 3H), 7.68–7.54 (m, 2H), 7.54–7.45

(m, 2H), 7.45–7.38 (m, 1H), 7.37–7.33 (m, 1H), 7.33–7.27 (m, 2H), 7.27–7.14 (m, 3H), 7.14–6.51 (m, 2H), 5.63–5.31 (m, 2H), 2.50–2.33 (m, 1H), 2.00–1.90 (m, 1H); ^{13}C NMR (101 MHz, DMSO-D_6) δ 159.05, 156.24, 155.23, 150.00, 138.13, 136.99, 135.17, 133.48, 130.53, 130.31, 129.41, 129.06, 128.65, 128.44, 127.97, 127.66, 127.49, 122.90, 121.45, 111.59, 103.55, 62.60, 49.80, 25.18, 18.56; HRMS-ESI$^+$ calculated for $C_{25}H_{23}ClN_5$ $[M + H]^+$ 428.1597, found: 428.1598.

4.1.21. (*Z*)-2-((*E*)-1-(1-Benzyl-1*H*-indol-3-yl)-3-(*o*-tolyl) allylidene)hydrazine-1-carboximidamide (1r). Synthesized as per the general procedure described above. Yield 87%, yellow solid. ^{1}H NMR (400 MHz, DMSO-D_6) δ 10.15 (s, 1H), 8.25–7.87 (m, 3H), 7.86–7.42 (m, 4H), 7.34 (ddd, J = 11.9, 7.5, 2.5 Hz, 4H), 7.29–7.19 (m, 4H), 7.19–7.07 (m, 3H), 7.01 (t, J = 12.7 Hz, 1H), 5.55 (d, J = 31.9 Hz, 2H), 2.26–1.82 (m, 3H); ^{13}C NMR (101 MHz, DMSO-D_6) δ 159.67, 156.02, 150.56, 138.09, 136.65, 136.43, 134.81, 131.65, 131.05, 129.60, 129.16, 129.08, 128.97, 128.05, 127.72, 127.51, 126.94, 126.14, 125.63, 122.85, 121.06, 120.23, 111.66, 103.82, 49.96, 19.57; HRMS-ESI$^+$ calculated for $C_{26}H_{26}N_5$ $[M + H]^+$ 408.2152, found: 408.2149.

4.1.22. (*Z*)-2-((*E*)-1-(1-(2,4-Difluorobenzyl)-1*H*-indol-3-yl)-3-phenylallylidene)hydrazine-1-carboximidamide (2a). Synthesized as per the general procedure described above. Yield 87%, yellow solid. ^{1}H NMR (400 MHz, DMSO-D_6) δ 8.83 (d, J = 23.3 Hz, 1H), 8.33–7.84 (m, 2H), 7.79–7.61 (m, 2H), 7.50 (ddd, J = 21.6, 12.0, 6.7 Hz, 2H), 7.39–7.17 (m, 5H), 7.14–6.91 (m, 3H), 5.63–5.31 (m, 2H), 4.03 (q, J = 7.1 Hz, 1H), 2.03–1.85 (m, 2H), 1.17 (t, J = 7.1 Hz, 1H); ^{13}C NMR (101 MHz, DMSO-D_6) δ 170.80, 159.63, 159.18, 156.43, 156.27, 151.52, 137.27, 133.13, 131.31, 128.49, 125.19, 123.71, 123.21, 121.60, 114.24, 112.33, 112.12, 110.58, 104.62, 60.23, 25.13, 21.24, 18.60, 16.59, 14.55; HRMS-ESI$^+$ calculated for $C_{25}H_{22}F_2N_5$ $[M + H]^+$ 430.1843, found: 430.1845.

4.1.23. (*Z*)-2-((*E*)-3-Phenyl-1-(1-(4-(trifluoromethyl)benzyl)-1*H*-indol-3-yl)allylidene)hydrazine-1-carboximidamide (2b). Synthesized as per the general procedure described above. Yield 91%, yellow solid. ^{1}H NMR (400 MHz, DMSO-D_6) δ 8.82 (d, J = 28.2 Hz, 1H), 8.26 (dd, J = 32.0, 19.4 Hz, 1H), 8.09–7.97 (m, 1H), 7.82 (s, 2H), 7.71 (s, 2H), 7.60 (d, J = 33.0 Hz, 2H), 7.48 (s, 1H), 7.40 (dd, J = 22.1, 7.2 Hz, 2H), 7.27 (s, 1H), 7.19 (s, 2H), 7.07–7.01 (m, 1H), 6.97–6.86 (m, 1H), 5.61 (dd, J = 50.9, 35.0 Hz, 2H), 4.69 (s, 1H), 2.00–1.84 (m, 2H); ^{13}C NMR (101 MHz, DMSO-D_6) δ 170.15, 163.93, 163.73, 159.62, 159.16, 158.79, 156.42, 156.27, 155.12, 151.60, 137.33, 133.38, 129.14, 128.62, 128.48, 128.10, 126.04, 123.22, 121.61, 114.26, 110.78, 49.30, 25.13, 21.21, 18.60, 16.61; HRMS-ESI$^+$ calculated for $C_{26}H_{23}F_3N_5$ $[M + H]^+$ 462.1906, found: 462.1910.

4.1.24. (*Z*)-2-((*E*)-1-(1-(3,5-Bis(trifluoromethyl)benzyl)-1*H*-indol-3-yl)-3-phenylallylidene)hydrazine-1-carboximidamide (2c). Synthesized as per the general procedure described above. Yield 84%, brown solid. ^{1}H NMR (400 MHz, DMSO-D_6) δ 9.00–8.22 (m, 2H), 8.19–8.07 (m, 1H), 8.04–7.80 (m, 3H), 7.58 (dd, J = 30.6, 22.8 Hz, 3H), 7.45–7.37 (m, 1H), 7.31–7.13 (m, 4H), 6.89 (d, J = 123.6 Hz, 2H), 6.12–5.34 (m, 2H), 4.85–4.44 (m, 1H), 2.43 (s, 1H), 1.99–1.89 (m, 1H); ^{13}C NMR (101 MHz, DMSO-D_6) δ 159.62, 156.47, 156.42, 156.29, 155.10, 151.51, 141.60, 137.22, 133.22, 131.10, 130.77, 129.13, 128.47, 127.35, 125.26, 123.84, 123.39, 121.96, 121.78, 114.53, 110.67, 48.76, 25.12, 21.21, 18.59, 16.61, 14.54; HRMS-ESI$^+$ calculated for $C_{27}H_{22}F_6N_5$ $[M + H]^+$ 530.1782, found: 530.1788.

4.1.25. (*Z*)-2-((*E*)-1-(1-(4-Fluoro-2-(trifluoromethyl)benzyl)-1*H*-indol-3-yl)-3-phenylallylidene)hydrazine-1-carboximidamide (2d). Synthesized as per the general procedure described above. Yield 88%, yellow solid. ^{1}H NMR (400 MHz, DMSO-D_6) δ 8.84 (d, J = 49.5 Hz, 2H), 8.39–7.87 (m, 1H), 7.90–6.30 (m, 14H), 4.96–3.98 (m, 2H), 1.99–1.84 (m, 2H); ^{13}C NMR (101 MHz, DMSO-D_6) δ 170.15, 169.90, 159.71, 159.24, 156.89, 156.51, 156.41, 156.37, 155.05, 151.36, 148.70, 137.31, 133.59, 129.41, 125.32, 123.50, 121.83, 120.53, 120.37, 117.11, 114.55, 43.44, 25.13, 21.23, 18.68, 16.69; HRMS-ESI$^+$ calculated for $C_{26}H_{22}F_4N_5$ $[M]^+$ 480.1811, found: 480.1814.

4.1.26. (*Z*)-2-((*E*)-1-(1-(2-Cyanobenzyl)-1*H*-indol-3-yl)-3-phenylallylidene)hydrazine-1-carboximidamide (2e). Synthesized as per the general procedure described above. Yield 93%, yellow solid. ^{1}H NMR (400 MHz, DMSO-D_6) δ 8.30–8.01 (m, 1H), 7.99–7.86 (m, 1H), 7.86–7.66 (m, 2H), 7.64–7.55 (m, 1H), 7.52–7.36 (m, 3H), 7.28 (ddd, J = 24.4, 18.8, 10.8 Hz, 3H), 7.20–7.14 (m, 1H), 7.13–7.06 (m, 1H), 6.97 (d, J = 15.2 Hz, 1H), 6.85–6.41 (m, 1H), 4.03 (q, J = 7.1 Hz, 1H), 3.37 (s, 2H), 2.06–1.87 (m, 1H), 1.29–1.08 (m, 2H), 0.96–0.79 (m, 1H); ^{13}C NMR (101 MHz, DMSO-D_6) δ 170.82, 156.16, 156.11, 155.77, 152.33, 137.59, 129.95, 129.38, 129.23, 128.91, 128.78, 128.69, 128.50, 128.40, 128.28, 128.05, 125.84, 124.60, 122.76, 121.04, 114.22, 112.14, 60.23, 21.21, 16.36, 14.56; HRMS-ESI$^-$ calculated for $C_{26}H_{21}N_6$ $[M - H]^+$ 417.1872, found: 417.1875.

4.1.27. (*Z*)-2-((*E*)-1-(1-(4-Chlorobenzyl)-1*H*-indol-3-yl)-3-phenylallylidene)hydrazine-1-carboximidamide (2f). Synthesized as per the general procedure described above. Yield 89%, light yellow solid. ^{1}H NMR (400 MHz, DMSO-D_6) δ 11.13 (s, 1H), 8.36–7.87 (m, 2H), 7.60 (d, J = 45.8 Hz, 4H), 7.53–7.47 (m, 1H), 7.40 (dt, J = 22.4, 10.2 Hz, 3H), 7.27 (d, J = 8.5 Hz, 2H), 7.23–6.94 (m, 3H), 5.48 (s, 2H), 2.42 (s, 3H), 2.00–1.89 (m, 1H); ^{13}C NMR (101 MHz, DMSO-D_6) δ 170.15, 159.58, 159.14, 156.39, 156.22, 151.65, 137.25, 137.09, 133.30, 132.76, 132.60, 129.47, 129.39, 129.16, 129.06, 125.30, 123.68, 123.12, 121.54, 114.08, 110.87, 49.13, 21.22, 18.58, 16.58; HRMS-ESI$^+$ calculated for $C_{25}H_{23}ClN_5$ $[M + H]^+$ 428.1774, found: 428.1779.

4.1.28. (*Z*)-2-((*E*)-1-(1-(3,5-Dimethoxybenzyl)-1*H*-indol-3-yl)-3-phenylallylidene)hydrazine-1-carboximidamide (2g). Synthesized as per the general procedure described above. Yield 82%, yellow solid. ^{1}H NMR (400 MHz, DMSO-D_6) δ 11.24–11.01 (m, 1H), 8.87 (s, 1H), 8.36–7.98 (m, 1H), 7.81 (d, J = 6.4 Hz, 1H), 7.63 (d, J = 15.8 Hz, 3H), 7.49 (dd, J = 15.0, 7.2 Hz, 1H), 7.27–7.10 (m, 7H), 6.59–6.28 (m, 2H), 5.57–5.16 (m, 1H), 3.87–3.51 (m, 6H), 2.41 (d, J = 3.8 Hz, 1H), 1.97 (d, J = 7.5 Hz, 2H); ^{13}C NMR (101 MHz, DMSO-D_6) δ 161.08, 159.63, 156.44, 156.26, 155.68, 155.09, 151.68, 140.35, 137.42, 133.44, 129.14, 128.44, 125.22, 123.61, 123.04, 121.46, 113.91, 110.95, 105.91, 105.81, 99.06, 55.65, 49.86, 25.13, 21.22, 18.63, 16.62; HRMS-ESI$^+$ calculated for $C_{27}H_{28}N_5O_2$ $[M + H]^+$ 454.2259, found: 454.2266.

4.1.29. (*Z*)-2-((*E*)-1-(1-(2-Fluorobenzyl)-1*H*-indol-3-yl)-3-phenylallylidene)hydrazine-1-carboximidamide (2h). Synthesized as per the general procedure described above. Yield 86%, yellow solid. ^{1}H NMR (400 MHz, DMSO-D_6) δ 11.27 (dd, J =

129.2, 47.1 Hz, 1H), 10.15 (d, J = 12.4 Hz, 1H), 9.56 (s, 1H), 8.88 (s, 1H), 8.17–7.87 (m, 1H), 7.83–7.75 (m, 1H), 7.66–7.60 (m, 1H), 7.57–7.49 (m, 1H), 7.49–7.40 (m, 1H), 7.35 (ddd, J = 9.6, 5.8, 3.3 Hz, 1H), 7.31–7.25 (m, 1H), 7.25–7.21 (m, 1H), 7.20–7.16 (m, 1H), 7.15–7.11 (m, 1H), 7.11–6.58 (m, 2H), 5.65–5.36 (m, 1H), 4.29–3.39 (m, 2H), 1.97 (d, J = 7.6 Hz, 1H), 1.89 (s, 2H); ^{13}C NMR (101 MHz, DMSO-D_6) δ 170.14, 159.64, 159.19, 156.45, 156.29, 155.08, 151.53, 137.34, 133.28, 130.39, 128.63, 128.48, 125.16, 123.69, 123.17, 121.56, 116.08, 115.87, 114.14, 110.62, 43.94, 25.13, 21.22, 18.64, 16.62; HRMS-ESI$^+$ calculated for $C_{25}H_{23}FN_5$ $[M + H]^+$ 412.1968, found: 412.1971.

4.1.30. (*Z*)-2-((*E*)-1-(1-(4-Bromo-2-fluorobenzyl)-1*H*-indol-3-yl)-3-phenylallylidene)hydrazine-1-carboximidamide (2i). Synthesized as per the general procedure described above. Yield 75%, yellow solid. ^{1}H NMR (400 MHz, DMSO-D_6) δ 11.11 (s, 1H), 8.36–7.93 (m, 2H), 7.68 (s, 2H), 7.65–7.56 (m, 2H), 7.54–7.42 (m, 2H), 7.36 (dt, J = 19.1, 9.5 Hz, 2H), 7.27–7.10 (m, 3H), 7.08–6.89 (m, 2H), 5.51 (s, 2H), 2.40 (s, 2H), 2.03–1.88 (m, 1H); ^{13}C NMR (101 MHz, DMSO-D_6) δ 161.47, 159.58, 158.98, 156.22, 151.53, 137.30, 133.20, 131.34, 131.30, 128.38, 128.35, 125.18, 124.57, 124.42, 123.73, 123.26, 121.71, 121.65, 119.54, 119.29, 114.30, 110.58, 60.23, 43.63, 16.56; HRMS-ESI$^+$ calculated for $C_{25}H_{22}BrFN_5$ $[M + H]^+$ 492.1217, found: 492.1218.

4.1.31. (*Z*)-2-((*E*)-1-(1-(3-Cyanobenzyl)-1*H*-indol-3-yl)-3-phenylallylidene)hydrazine-1-carboximidamide (2j). Synthesized as per the general procedure described above. Yield 78%, yellow solid. ^{1}H NMR (400 MHz, DMSO-D_6) δ 11.56–10.98 (m, 1H), 8.97–8.65 (m, 1H), 8.38–8.08 (m, 1H), 8.04–7.89 (m, 1H), 7.89–7.70 (m, 2H), 7.59 (dd, J = 27.8, 19.2 Hz, 2H), 7.45 (ddd, J = 26.5, 14.9, 6.5 Hz, 2H), 7.36–7.26 (m, 1H), 7.25–7.10 (m, 2H), 7.04 (t, J = 23.3 Hz, 2H), 6.96–6.45 (m, 1H), 5.53 (dd, J = 41.5, 22.0 Hz, 1H), 4.85–4.12 (m, 2H), 3.14 (d, J = 22.4 Hz, 1H), 2.38 (d, J = 32.5 Hz, 1H), 2.00–1.88 (m, 1H); ^{13}C NMR (101 MHz, DMSO-D_6) δ 167.47, 159.65, 158.82, 156.45, 156.29, 155.65, 155.08, 148.74, 146.79, 138.70, 137.32, 136.98, 133.35, 131.58, 129.43, 129.14, 128.93, 128.75, 128.45, 128.19, 128.10, 49.04, 25.13, 18.64, 16.64, 14.60; HRMS-ESI$^+$ calculated for $C_{26}H_{23}N_6$ $[M + H]^+$ 419.1925, found: 419.1921.

4.1.32. (*Z*)-2-((*E*)-1-(1-(4-(Trifluoromethyl)benzyl)-1*H*-indol-3-yl)-3-(4-(trifluoromethyl)phenyl)allylidene)hydrazine-1-carboximidamide (3a). Synthesized as per the general procedure described above. Yield 92%, yellow solid. ^{1}H NMR (400 MHz, DMSO-D_6) δ 10.12 (d, J = 24.0 Hz, 1H), 9.57 (s, 1H), 8.97 (d, J = 24.6 Hz, 1H), 8.14 (t, J = 84.0 Hz, 1H), 7.85–7.65 (m, 3H), 7.64–7.48 (m, 2H), 7.48–7.37 (m, 1H), 7.27 (s, 3H), 7.16 (dd, J = 17.6, 8.2 Hz, 2H), 4.01 (s, 2H), 2.06–1.70 (m, 4H); ^{13}C NMR (101 MHz, DMSO-D_6) δ 170.17, 159.67, 159.58, 159.23, 159.18, 156.45, 156.30, 155.67, 155.11, 151.57, 148.75, 142.91, 137.27, 133.49, 128.68, 128.11, 125.99, 125.26, 123.71, 123.21, 121.61, 114.23, 110.81, 25.13, 21.22, 18.64, 16.66; HRMS-ESI$^+$ calculated for $C_{27}H_{22}$ F_6N_5 $[M + H]^+$ 530.1742, found: 530.1745.

4.1.33. (*Z*)-2-((*E*)-1-(1-(3,5-Dimethoxybenzyl)-1*H*-indol-3-yl)-3-(3,4-dimethoxyphenyl)allylidene)hydrazine-1-carboximidamide (3b). Synthesized as per the general procedure described above. Yield 75%, yellow solid. ^{1}H NMR (400 MHz, DMSO-D_6) δ 11.06 (dd, J = 42.7, 13.8 Hz, 1H), 10.13 (s, 1H), 9.56 (s, 1H), 8.87 (s, 1H), 8.30–8.18 (m, 1H), 7.72 (s, 1H), 7.65 (s, 1H), 7.50 (dt, J = 26.1, 11.7 Hz, 2H), 7.17 (ddd, J = 14.9, 14.0, 7.0 Hz, 4H), 6.39 (s, 2H), 5.38 (s, 1H), 3.91–3.45 (m, 12H), 1.97–1.89 (m, 3H); ^{13}C NMR (101 MHz, DMSO-D_6) δ 170.19, 170.16, 161.07, 159.74, 159.62, 159.17, 156.43, 156.25, 155.11, 151.69, 148.76, 140.34, 137.41, 133.45, 125.21, 123.61, 123.04, 121.46, 113.89, 110.95, 105.84, 105.80, 99.05, 55.65, 49.86, 25.13, 21.22, 18.63, 16.62; HRMS-ESI$^+$ calculated for $C_{29}H_{32}N_5O_4$ $[M + H]^+$ 514.2412, found: 514.2409.

4.1.34. (*Z*)-2-((*E*)-1-(1-([1,1′-Biphenyl]-4-ylmethyl)-1*H*-indol-3-yl)-3-(4-(*tert*-butyl)phenyl)allylidene)hydrazine-1-carboximidamide (3c). Synthesized as per the general procedure described above. Yield 82%, yellowish brown solid. ^{1}H NMR (400 MHz, DMSO-D_6) δ 11.09 (d, J = 49.2 Hz, 1H), 8.86 (s, 1H), 8.36–7.93 (m, 3H), 7.60 (d, J = 8.0 Hz, 5H), 7.53 (d, J = 8.0 Hz, 1H), 7.43 (t, J = 7.6 Hz, 3H), 7.35 (d, J = 2.5 Hz, 1H), 7.33 (d, J = 1.3 Hz, 1H), 7.32 (d, J = 3.6 Hz, 1H), 7.18 (ddd, J = 14.9, 14.0, 6.9 Hz, 3H), 5.52 (s, 2H), 4.72 (s, 1H), 3.42 (s, 9H), 2.43 (s, 1H), 1.98–1.90 (m, 2H); ^{13}C NMR (101 MHz, DMSO-D_6) δ 170.16, 159.61, 159.44, 159.16, 156.42, 156.24, 155.65, 155.11, 151.69, 148.77, 140.11, 139.87, 137.37, 137.26, 133.40, 129.36, 128.16, 128.09, 127.93, 127.37, 127.07, 125.31, 123.67, 123.08, 121.49, 113.99, 110.97, 56.48, 49.54, 25.13, 21.22, 19.03, 18.68, 18.60, 16.62; HRMS-ESI$^+$ calculated for $C_{35}H_{36}N_5$ $[M + H]^+$ 526.2931, found: 526.2928.

4.1.35. (*Z*)-2-((*E*)-1-(1-(4-(*tert*-Butyl)benzyl)-1*H*-indol-3-yl)-3-(3,4-difluorophenyl)allylidene)hydrazine-1-carboximidamide (3d). Synthesized as per the general procedure described above. Yield 87%, yellow solid. ^{1}H NMR (400 MHz, DMSO-D_6) δ 11.09 (d, J = 54.1 Hz, 1H), 10.14 (s, 1H), 9.56 (s, 1H), 8.87 (s, 1H), 8.15 (s, 1H), 7.82 (s, 1H), 7.66 (s, 1H), 7.32 (d, J = 2.5 Hz, 1H), 7.30–7.28 (m, 1H), 7.27–7.25 (m, 1H), 7.24 (d, J = 1.2 Hz, 1H), 7.22 (s, 1H), 7.20 (d, J = 1.4 Hz, 1H), 7.18–7.17 (m, 1H), 7.14 (d, J = 7.0 Hz, 1H), 7.07–7.02 (m, 1H), 5.50 (s, 2H), 2.39 (s, 2H), 1.99–1.85 (m, 9H); ^{13}C NMR (101 MHz, DMSO-D_6) δ 170.17, 159.62, 159.17, 156.43, 156.27, 155.66, 155.11, 151.51, 148.76, 137.24, 133.15, 131.33, 125.16, 123.70, 123.20, 121.60, 121.26, 114.19, 112.37, 112.15, 110.58, 104.88, 104.62, 43.51, 25.13, 21.22, 18.68, 18.63, 16.62; HRMS-ESI$^+$ calculated for $C_{29}H_{30}$ F_2N_5 $[M + H]^+$ 486.2408, found: 486.2411.

4.1.36. (*Z*)-2-((*E*)-3-(4-(Benzyloxy)phenyl)-1-(1-(4-methylbenzyl)-1*H*-indol-3-yl)allylidene)hydrazine-1-carboximidamide (3e). Synthesized as per the general procedure described above. Yield 83%, yellow solid. ^{1}H NMR (400 MHz, DMSO-D_6) δ 11.07 (d, J = 45.9 Hz, 1H), 10.12 (s, 1H), 9.55 (s, 1H), 8.29–8.19 (m, 1H), 7.65 (s, 1H), 7.55–7.51 (m, 2H), 7.47 (d, J = 5.4 Hz, 1H), 7.45 (s, 2H), 7.40 (t, J = 7.5 Hz, 3H), 7.34 (dd, J = 7.1, 1.5 Hz, 1H), 7.19–7.15 (m, 2H), 7.11 (d, J = 8.1 Hz, 2H), 6.96 (d, J = 8.6 Hz, 1H), 6.33 (s, 1H), 5.42 (d, J = 13.1 Hz, 2H), 5.07 (d, J = 5.7 Hz, 2H), 2.41 (s, 1H), 2.24 (s, 1H), 1.98–1.95 (m, 2H), 1.90 (s, 3H); ^{13}C NMR (101 MHz, DMSO-D_6) δ 170.14, 159.60, 159.16, 158.52, 156.42, 156.23, 155.10, 151.70, 137.47, 137.30, 137.18, 135.00, 133.33, 130.22, 129.59, 128.89, 128.32, 128.29, 127.54, 125.28, 123.60, 122.97, 121.40, 114.55, 113.82, 110.96, 69.71, 49.69, 25.13, 21.22, 21.12, 18.61, 16.59; HRMS-ESI$^+$ calculated for $C_{33}H_{32}N_5O$ $[M + H]^+$ 514.2554, found: 514.2559.

4.1.37. (*Z*)-2-((*E*)-1-(1-(2,5-Difluorobenzyl)-1*H*-indol-3-yl)-3-(4-isopropylphenyl)allylidene)hydrazine-1-carboximidamide (3f). Synthesized as per the general procedure described above. Yield 93%, yellow solid. ^{1}H NMR (400 MHz, DMSO-D$_6$) δ 11.17 (s, 1H), 10.13 (s, 1H), 9.56 (s, 1H), 8.88 (s, 1H), 8.30–8.17 (m, 1H), 7.81 (d, J = 9.9 Hz, 1H), 7.66 (s, 1H), 7.52 (dd, J = 9.5, 4.4 Hz, 2H), 7.34–7.27 (m, 2H), 7.25–7.23 (m, 1H), 7.21 (d, J = 1.3 Hz, 1H), 7.19 (d, J = 4.4 Hz, 1H), 7.16 (dd, J = 9.3, 2.3 Hz, 1H), 6.95 (ddd, J = 8.9, 5.6, 3.2 Hz, 1H), 5.52 (s, 2H), 4.04–3.92 (m, 1H), 2.40 (s, 2H), 1.98–1.89 (m, 6H); ^{13}C NMR (101 MHz, DMSO-D$_6$) δ 170.14, 159.72, 159.62, 159.18, 156.44, 156.29, 155.08, 151.50, 148.74, 137.24, 133.19, 125.14, 123.73, 123.28, 121.66, 117.77, 117.53, 116.82, 116.67, 116.38, 116.13, 114.32, 110.56, 43.76, 25.13, 21.22, 18.63, 16.62; HRMS-ESI$^+$ calculated for $C_{28}H_{28}F_2N_5$ [M + H]$^+$ 472.2274, found: 472.2270.

4.1.38. (*Z*)-2-((*E*)-1-(1-(4-Bromobenzyl)-1*H*-indol-3-yl)-3-(4-(*tert*-butyl)phenyl)allylidene)hydrazine-1-carboximidamide (3g). Synthesized as per the general procedure described above. Yield 76%, yellow solid. ^{1}H NMR (400 MHz, DMSO-D$_6$) δ 11.16 (s, 1H), 8.86 (s, 1H), 8.28 (d, J = 7.4 Hz, 1H), 8.23 (s, 1H), 7.65 (s, 1H), 7.52 (d, J = 8.4 Hz, 3H), 7.46 (d, J = 7.6 Hz, 1H), 7.21 (s, 2H), 7.19 (s, 2H), 7.17 (dd, J = 3.9, 1.2 Hz, 1H), 7.14 (d, J = 6.9 Hz, 1H), 5.46 (s, 2H), 4.57 (d, J = 101.4 Hz, 3H), 3.33 (dd, J = 88.1, 6.9 Hz, 6H), 2.41 (s, 3H), 1.98–1.96 (m, 1H); ^{13}C NMR (101 MHz, DMSO-D$_6$) δ 159.62, 156.43, 156.36, 156.34, 156.26, 155.09, 151.67, 151.61, 137.51, 137.47, 137.32, 137.24, 133.31, 131.97, 129.82, 129.72, 125.29, 123.74, 123.69, 123.12, 121.54, 121.11, 114.08, 110.87, 49.18, 25.14, 18.69, 18.62, 16.62; HRMS-ESI$^+$ calculated for $C_{29}H_{31}BrN_5$ [M + H]$^+$ 528.1763, found: 530.1689.

4.1.39. (*Z*)-2-((*E*)-1-(1-(4-(*tert*-Butyl)benzyl)-1*H*-indol-3-yl)-3-(4-(*tert*-butyl)phenyl)allylidene)hydrazine-1-carboximidamide (3h). Synthesized as per the general procedure described above. Yield 81%, yellow solid. ^{1}H NMR (400 MHz, DMSO-D$_6$) δ 11.11 (d, J = 47.1 Hz, 1H), 10.14 (s, 1H), 9.56 (s, 1H), 8.92 (s, 2H), 8.24 (d, J = 10.2 Hz, 1H), 7.66 (s, 2H), 7.51 (d, J = 8.0 Hz, 1H), 7.33 (s, 1H), 7.31 (s, 1H), 7.25 (s, 3H), 7.19 (s, 1H), 7.16 (d, J = 7.6 Hz, 1H), 7.12 (d, J = 7.0 Hz, 1H), 5.42 (s, 2H), 2.41 (s, 2H), 1.98–1.89 (m, 9H), 1.30–1.15 (m, 9H); ^{13}C NMR (101 MHz, DMSO-D$_6$) δ 170.14, 159.70, 159.68, 159.61, 159.19, 156.46, 156.27, 155.07, 151.66, 150.37, 137.34, 135.11, 133.33, 127.31, 127.26, 127.21, 125.85, 125.79, 125.48, 125.23, 123.60, 123.00, 121.40, 113.86, 110.94, 49.49, 34.66, 31.52, 25.13, 21.22, 18.68, 18.65, 16.64; HRMS-ESI$^+$ calculated for $C_{33}H_{40}N_5$ [M + H]$^+$ 506.3284, found: 506.3284.

4.1.40. (*Z*)-2-((*E*)-1-(1-(3-(Benzyloxy)benzyl)-1*H*-indol-3-yl)-3-(4-(benzyloxy)phenyl)allylidene)hydrazine-1-carboximidamide (3i). Synthesized as per the general procedure described above. Yield 87%, yellow solid. ^{1}H NMR (400 MHz, DMSO-D$_6$) δ 11.30–10.95 (m, 1H), 10.10 (d, J = 27.4 Hz, 1H), 9.51 (d, J = 49.3 Hz, 1H), 8.84 (d, J = 59.6 Hz, 2H), 8.33–7.87 (m, 2H), 7.74 (dd, J = 32.5, 23.8 Hz, 4H), 7.53 (dd, J = 7.9, 5.7 Hz, 1H), 7.49–7.43 (m, 2H), 7.39 (dd, J = 10.2, 4.2 Hz, 2H), 7.36–7.31 (m, 2H), 7.31–7.22 (m, 4H), 7.21–7.12 (m, 2H), 7.05 (dd, J = 28.6, 8.2 Hz, 1H), 6.98–6.89 (m, 2H), 6.81 (d, J = 7.6 Hz, 1H), 5.54–5.31 (m, 1H), 5.14–4.99 (m, 2H), 4.66 (s, 2H), 2.41 (s, 1H), 1.98–1.89 (m, 2H); ^{13}C NMR (101 MHz, DMSO-D$_6$) δ 170.13, 159.62, 159.20, 158.93, 158.50, 156.46, 156.28, 155.06, 154.46, 151.66, 139.65, 137.47, 137.43, 137.36, 137.30, 133.38, 130.23, 128.92, 128.89, 128.86, 128.33, 128.31, 128.25, 125.25, 123.62, 123.04, 121.45, 119.87, 114.50, 114.41, 113.92, 113.83, 110.93, 69.63, 49.76, 25.13, 21.23, 18.64, 16.64; HRMS-ESI$^+$ calculated for $C_{39}H_{36}N_5O_2$ [M + H]$^+$ 606.2905, found: 606.2909.

4.1.41. (*Z*)-2-((*E*)-1-(1-(4-Butylbenzyl)-1*H*-indol-3-yl)-3-(4-(trifluoromethyl)phenyl)allylidene)hydrazine-1-carboximidamide (3j). Synthesized as per the general procedure described above. Yield 87%, white solid. ^{1}H NMR (400 MHz, DMSO-D$_6$) δ 11.14 (s, 1H), 8.86 (s, 1H), 8.33–8.10 (m, 2H), 7.66 (s, 4H), 7.55–7.42 (m, 2H), 7.19 (dd, J = 10.7, 3.8 Hz, 2H), 7.15 (s, 2H), 7.13 (d, J = 3.2 Hz, 2H), 7.11 (s, 1H), 5.41 (s, 2H), 2.41 (s, 2H), 1.99–1.86 (m, 2H), 1.53–1.39 (m, 2H), 1.30–1.15 (m, 2H), 0.84 (t, J = 7.3 Hz, 3H); ^{13}C NMR (101 MHz, DMSO-D$_6$) δ 170.15, 159.62, 159.17, 156.43, 156.24, 155.10, 151.69, 142.10, 137.33, 135.27, 133.33, 128.99, 128.93, 127.59, 127.49, 125.26, 123.60, 122.99, 121.41, 113.84, 110.94, 49.65, 34.88, 33.55, 25.13, 22.18, 21.22, 18.62, 16.61, 14.20; HRMS-ESI$^+$ calculated for $C_{30}H_{31}F_3N_5$ [M + H]$^+$ 518.2569, found: 518.2573.

4.1.42. (*Z*)-2-((*E*)-3-(4-(*tert*-Butyl)phenyl)-1-(1-(4-(trifluoromethyl)benzyl)-1*H*-indol-3-yl)allylidene)hydrazine-1-carboximidamide (3k). Synthesized as per the general procedure described above. Yield 75%, yellow solid. ^{1}H NMR (400 MHz, DMSO-D$_6$) δ 11.03 (d, J = 16.9 Hz, 1H), 8.87 (d, J = 14.8 Hz, 1H), 7.79–7.59 (m, 3H), 7.54–7.46 (m, 1H), 7.33–7.26 (m, 2H), 7.23–7.17 (m, 1H), 7.16–7.10 (m, 2H), 7.09–7.04 (m, 1H), 7.00 (d, J = 8.7 Hz, 2H), 6.77–6.71 (m, 1H), 6.20 (ddd, J = 6.5, 5.1, 2.9 Hz, 1H), 5.66–5.53 (m, 2H), 3.86–3.40 (m, 9H), 2.22 (s, 1H), 1.94 (dd, J = 25.7, 8.1 Hz, 2H); ^{13}C NMR (101 MHz, DMSO-D$_6$) δ 170.13, 159.60, 159.16, 156.41, 156.32, 156.16, 155.09, 153.01, 147.74, 147.65, 147.60, 139.49, 129.24, 128.91, 128.86, 128.67, 128.26, 121.77, 121.58, 121.48, 119.23, 116.32, 108.59, 61.31, 56.22, 51.90, 25.13, 21.21, 18.60, 16.98; HRMS-ESI$^+$ calculated for $C_{30}H_{30}F_3N_5Na$ [M + Na]$^+$ 540.2251, found: 540.2244.

4.1.43. (*Z*)-2-((*E*)-1-(1-(4-Butylbenzyl)-1*H*-indol-3-yl)-3-(2,5-dimethoxyphenyl)allylidene)hydrazine-1-carboximidamide (3l). Synthesized as per the general procedure described above. Yield 93%, yellow solid. ^{1}H NMR (400 MHz, DMSO-D$_6$) δ 11.17 (s, 1H), 8.93 (s, 2H), 8.29–8.20 (m, 2H), 7.69 (d, J = 14.9 Hz, 1H), 7.49 (d, J = 8.0 Hz, 1H), 7.26 (s, 5H), 7.20 (dd, J = 7.1, 1.1 Hz, 1H), 7.17 (d, J = 1.0 Hz, 1H), 7.15 (s, 1H), 7.13 (s, 1H), 7.12–7.10 (m, 1H), 5.41 (s, 2H), 4.39 (d, J = 87.6 Hz, 6H), 2.48 (s, 1H), 2.41 (s, 2H), 1.52–1.42 (m, 2H), 1.31–1.18 (m, 2H), 0.85 (t, J = 7.3 Hz, 3H); ^{13}C NMR (101 MHz, DMSO-D$_6$) δ 159.59, 156.32, 156.26, 156.22, 151.66, 142.14, 142.09, 137.41, 137.33, 135.34, 135.28, 133.39, 133.32, 129.01, 128.93, 127.57, 127.49, 125.30, 125.26, 123.61, 122.98, 121.40, 113.85, 111.01, 110.94, 49.64, 34.89, 33.55, 22.18, 16.63, 14.20; HRMS-ESI$^+$ calculated for $C_{31}H_{39}N_6O_2$ [M + NH$_4$]$^+$; 527.3157, found: 527.3162.

4.2. AChE inhibition assay

The inhibitory effects of 102 compounds on EeAChE were assessed using a modified Ellman assay at concentrations of 10–4 M and 10–5 M. *Electrophorus electricus* acetylcholinesterase (EeAChE, EC 3.1.1.7, from electric eel, type V–S, 827 U mg^{-1} solid; 1256 U mg^{-1} of protein), acetylthiocholine iodide (ATChI), 5,5-dithiobis-(2-nitrobenzoic acid) (DTNB, Ellman

reagent), donepezil were purchased from Sigma-Aldrich. Molecular biology grade DMSO from Sigma was used for biological assays. Each compound was accurately weighed and dissolved in molecular biology grade DMSO to create a 10 mM stock solution. AChE was dissolved in 0.1 M phosphate buffer (pH 7.2) to prepare enzyme stock solutions at 1 mg mL^{-1} concentration, which were then further diluted with PBS to yield working solutions with enzyme activity of 2.5 units per mL. Working solutions of DTNB and ATChI were also prepared in PBS at concentrations of 0.3 mM, 10 mM, and 10 mM respectively. Test compound concentrations ranging from 1 to 100 μM were prepared from the stock solutions by dilution with PBS. In the experimental procedure, 20 μL of enzyme solution (AChE), 20 μL of test compound solution (inhibitor), and 140 μL of 0.3 mM DTNB solution were added to each well of a 96-well plate. Control wells contained the same components as the test wells, with the addition of the proportion of DMSO present in the test compound solution to account for any interference from DMSO. The assay solutions, with and without inhibitor, were pre-incubated at 25 °C for 20 minutes before the addition of 20 μL of 10 mM ATChI solution. The reaction was monitored by measuring absorbance at 412 nm at 1 minute intervals for a total of 10 minutes using a 96-well microplate reader, as the absorbance is directly proportional to enzymatic activity. Each experiment was performed in triplicate, and donepezil was used as the reference standard. Blank solutions, containing all components except enzyme solution, were prepared alongside the test solutions to account for nonenzymatic substrate hydrolysis. Percent inhibition values were calculated from the slopes of absorbance readings over different time intervals for both control and test compounds. IC_{50} values were determined graphically from the observed percentage inhibition values at different inhibitor concentrations using GraphPad Prism 8 software and are reported as mean ± SD (an average of three experiments).

4.3. BACE 1 inhibition assay

The BACE 1 fluorescence resonance energy transfer (FRET) assay kit, obtained from Sigma-Aldrich (Product No. CS0010, Saint Louis), was used following the manufacturer's protocol. Molecular biology grade DMSO from Sigma was used for biological assays. A stock solution of the substrate (500 μM) was prepared using DMSO, and aliquots were stored at −20 °C. Test compounds were dissolved in DMSO to create a 10 mM stock solution, and desired concentrations were achieved through further dilutions with fluorescent assay buffer (FAB, 50 mM sodium acetate buffer, pH 4.5) provided in the kit. Just before starting the assay, a BACE 1 enzyme solution (0.3 unit per μL) and a 50 μM substrate solution were prepared by dilution with FAB. The fluorometer was configured in well plate reader mode with excitation set at 320 nm and emission at 405 nm. For the assay, 10 μL of the test compound, 20 μL of substrate, and 68 μL of FAB were added to each well of a 96-well black polystyrene microplate. Two microliters of BACE 1 were then added, and fluorescence was immediately measured after enzyme addition. Following the initial reading ("time zero"), the plate was covered and incubated for 2 hours at 37 °C. After the incubation period, fluorescence intensities were measured again. The difference between the fluorescence readings at "time zero" and after 2 hours provided Δfluorescence, which was used for subsequent calculations. Each concentration was assayed in triplicate. The background signal was determined in control wells containing all reagents except BACE 1 and was subsequently subtracted. Fluorescence intensities of assay solutions without inhibitor were also measured. The percentage of inhibition due to the presence of test compound was calculated by the following expression: $100 - (I_{Fi}/I_{Fo} \times 100)$ where I_{Fi} and I_{Fo} are the respective fluorescence intensities obtained in the presence and in the absence of inhibitor. Percentage inhibition of enzyme by the compounds are reported as mean ± SD (an average of three experiments). BACE 1 inhibitor IV (Calbiochem IV; CAS no. 797035-11-1) (IC_{50} = 18 nM; literature value. 15 nM) were used as reference compounds.

4.4. Computational studies

4.4.1. *In silico* docking simulations. RCSB Protein Data Bank (PDB) (https://www.rcsb.org) was used to retrieve the crystal structures (PDB ID: 4EY7 for AChE, and 6UWP for BACE 1). Protein complex structures were created using the Protein Preparation Wizard (Schrödinger) and ligands were created using the LigPrep module. Using the OPLS_2005 force field, the low-energy conformers of ligand were computed. Hydrogen atoms and water molecules were removed and supplied separately throughout the protein production process. Within an orthorhombic box that stretched 20 Å in each direction, each grid box was formed according to the crystal ligands. Molecular dockings [extra-precision (XP)] were carried out with the Glide module implemented in Schrödinger 2022. The best docking poses determined by examining the interaction with key residues were output among the docking poses.

4.4.2. Molecular dynamics. To confirm the binding strength and pattern of the compound in AChE and BACE 1 complex using Desmond, a molecular dynamics simulation run of 100 ns was conducted. The clear-cut water environment was created by soaking the ligand–protein complex in the TIP3P molecules of water encompassed by the orthorhombic water box. The prepared complex system was neutralized by adding the necessary counter ions, and the isosmotic salt environment was maintained by adding 0.15 M NaCl. The system's energy minimization was achieved by using a combined gradient algorithm with maximal 2000 interactions with convergence criteria of 1 kcal mol^{-1} A^{-1}. Simulation run of 100 ns with periodic boundary conditions under isothermal-isobaric ensemble (NPT) was performed after energy minimization, and the system temperature and pressure were set respectively at 310 K and 1.013 atmospheric bar.

4.4.3. *In silico* determination of drug-like properties. Using Schrodinger Maestro's QikProp module 2022-1, the features of drug-likeliness were discovered. The properties of drug-likeliness in the molecule were determined by predicting many descriptors, such as molecular weight of the compound (Mol_Wt), hydrogen bond donor in a molecule (donor HB),

hydrogen bond acceptor with in a molecule (acceptor HB), SASA-total solvent accessible surface area (SASA) in square angstroms using a probe with a 1.4 Å radius, predicted brain/blood partition coefficient (QplogBB), predicted octanol/water (Qplogo/w).[29]

4.5. Statistical analysis

The experimental results were provided as mean standard deviation (±S.D.) GraphPad Prism 8.0 was used to analyze the data.

Data availability

The authors confirm that the data supporting the findings of this study are available within the article and/or its ESI materials.†

Author contributions

Amit Sharma collated the literature, carried out design and synthesis, and wrote the manuscript. Ankita Sharma and Sandip B. Bharate planned and carried out the screening and statistical analysis, Santosh Rudrawar and Hemant R. Jadhav conceptualized, monitored, reviewed, and supervised the entire work.

Conflicts of interest

The authors declare that they have no known competing financial interests or personal relationships that could have appeared to influence the work reported in this paper.

Acknowledgements

For conducting NMR and MASS experiments, the authors gratefully acknowledge the Central Instrument Facility (CIF), Birla Institute of Technology and Sciences (BITS) Pilani, Pilani Campus.

References

1 Z. Sang, K. Wang, J. Dong and L. Tang, Alzheimer's Disease: Updated Multi-targets Therapeutics Are in Clinical and in Progress, *Eur. J. Med. Chem.*, 2022, **238**, 114464.
2 **https://www.who.int**, accessed on 04-04-2024.
3 Z. Luo, J. Sheng, Y. Sun, C. Lu, J. Yan, A. Liu, H.-b. Luo, L. Huang and X. Li, Synthesis and evaluation of multi-target-directed ligands against Alzheimer's disease based on the fusion of donepezil and ebselen, *J. Med. Chem.*, 2013, **56**, 9089–9099.
4 P. Srivastava, P. N. Tripathi, P. Sharma and S. K. Shrivastava, Design, Synthesis, and Evaluation of Novel N-(4-phenoxybenzyl)Aniline Derivatives Targeting Acetylcholinesterase, β-amyloid Aggregation and Oxidative Stress to Treat Alzheimer'S Disease, *Bioorg. Med. Chem.*, 2019, **27**, 3650–3662.
5 J. Cummings, G. Lee, T. Mortsdorf, A. Ritter and K. Zhong, Alzheimer's Disease Drug Development Pipeline: 2017, *Alzheimer's Dement.: Transl. Res. Clin. Interv.*, 2017, **3**, 367–384.
6 R. E. Becker, N. H. Greig and E. Giacobini, Why do so many drugs for Alzheimer's disease fail in development? Time for new methods and new practices?, *J. Alzheimer's Dis.*, 2008, **15**, 303–325.
7 G. R. Langley, Considering a New Paradigm for Alzheimer's Disease Research, *Drug Discovery Today*, 2014, **19**, 1114–1124.
8 R. Anand, K. D. Gill and A. A. Mahdi, Therapeutics of Alzheimer's Disease: Past, Present and Future, *Neuropharmacology*, 2013, **76**, 27–50.
9 M. G. Savelieff, G. Nam, J. Kang, H. J. Lee, M. Lee and M. H. Lim, Development of multifunctional molecules as potential therapeutic candidates for Alzheimer's disease, Parkinson's disease, and amyotrophic lateral sclerosis in the last Decade, *Chem. Rev.*, 2018, **119**, 1221–1322.
10 A. Cavalli, M. L. Bolognesi, A. Minarini, M. Rosini, V. Tumiatti, M. Recanatini and C. Melchiorre, Multi-target-directed ligands to combat neurodegenerative diseases, *J. Med. Chem.*, 2008, **51**, 347–372.
11 O. Benek, J. Korabecny and O. Soukup, A perspective on multi-target drugs for Alzheimer's disease, *Trends Pharmacol. Sci.*, 2020, **41**, 434–445.
12 J. F. González, A. R. Alcántara and A. L. Doadrio, Jose María Sánchez- Montero, Developments with multi-target drugs for Alzheimer's disease: An overview of the current discovery approaches, *Expert Opin. Drug Discovery*, 2019, **14**, 879–891.
13 X. Du, X. Wang and M. Geng, Alzheimer's disease hypothesis and related therapies, *Transl. Neurodegener.*, 2018, **7**, 1–7.
14 L. A. Craig, N. S. Hong and R. J. McDonald, Revisiting the Cholinergic Hypothesis in the Development of Alzheimer's Disease, *Neurosci. Biobehav. Rev.*, 2011, **35**, 1397–1409.
15 H. Hampel, M.-M. Mesulam, A. Claudio Cuello, M. R. Farlow, E. Giacobini, G. T. Grossberg and A. S. Khachaturian, The cholinergic system in the pathophysiology and treatment of Alzheimer's disease, *Brain*, 2018, **141**, 1917–1933.
16 M. Bartolini, C. Bertucci, V. Cavrini and V. Andrisano, β-Amyloid Aggregation Induced by Human Acetylcholinesterase: Inhibition Studies, *Biochem. Pharmacol.*, 2003, **65**, 407–416.
17 R. M. Lane and S. G. Potkin, Albert Enz, Targeting acetylcholinesterase and butyrylcholinesterase in dementia, *Int. J. Neuropsychopharmacol.*, 2006, **9**, 101–124.
18 A. Alvarez, R. Alarcon, C. Opazo, E. O. Campos, F. Jose Munoz, F. H. Calderon and F. Dajas, Stable complexes involving acetylcholinesterase and amyloid-β peptide change the biochemical properties of the enzyme and increase the neurotoxicity of Alzheimer's fibrils, *J. Neurosci.*, 1998, **18**, 3213–3223.
19 B.-M. Swahn, K. Kolmodin, S. Karlström, S. von Berg, P. Söderman, J. Holenz and S. Berg, Design and synthesis of β-site amyloid precursor protein cleaving enzyme (BACE1) inhibitors with *in vivo* brain reduction of β-amyloid peptides, *J. Med. Chem.*, 2012, **55**, 9346–9361.

20 P. N. Nirmalraj, J. List, S. Battacharya, G. Howe, L. Xu, D. Thompson and M. Mayer, Complete aggregation pathway of amyloid β (1-40) and (1-42) resolved on an atomically clean interface, *Sci. Adv.*, 2020, **6**, eaaz6014.

21 M. Vaz, V. Silva, C. Monteiro and S. Silvestre, Role of aducanumab in the treatment of Alzheimer's disease: Challenges and opportunities, *Clin. Interventions Aging*, 2022, 797–810.

22 P. Sharma, A. Tripathi, P. N. Tripathi, S. K. Prajapati, A. Seth, M. K. Tripathi, P. Srivastava, V. Tiwari, S. Krishnamurthy and S. K. Shrivastava, Design and Development of Multitarget-directed N- Benzylpiperidine Analogs as Potential Candidates for the Treatment of Alzheimer's Disease, *Eur. J. Med. Chem.*, 2019, **167**, 510–524.

23 E. A. Dutysheva, I. A. Utepova, M. A. Trestsova, A. S. Anisimov, V. N. Charushin, O. N. Chupakhin, B. A. Margulis, I. V. Guzhova and V. F. Lazarev, Synthesis and Approbation of New Neuroprotective Chemicals of Pyrrolyl- and Indolylazine Classes in a Cell Model of Alzheimer's Disease, *Eur. J. Med. Chem.*, 2021, **222**, 113577.

24 P. Jain, P. K. Wadhwa, S. Rohilla and H. R. Jadhav, Rational Design, Synthesis and in Vitro Evaluation of Allylidene Hydrazinecarboximidamide Derivatives as BACE-1 Inhibitors, *Bioorg. Med. Chem. Lett.*, 2015, **26**, 33–37.

25 A. Sharma and S. B. Bharate, Synthesis and biological evaluation of coumarin triazoles as dual inhibitors of cholinesterases and β-secretase, *ACS Omega*, 2023, **8**, 11161–11176.

26 Y. Zhao, F. Ye, J. Xu, Q. Liao, L. Chen, W. Zhang, H. Sun, W. Liu, F. Feng and W. Qu, Design, Synthesis and Evaluation of Novel Bivalent β-carboline Derivatives as Multifunctional Agents for the Treatment of Alzheimer's Disease, *Bioorg. Med. Chem.*, 2018, **26**, 3812–3824.

27 Q. Liao, L. Qi, Y. Zhao, P. Jiang, Y. Yan, H. Sun, W. Liu, F. Feng and W. Qu, Design, Synthesis and Biological Evaluation of Novel Carboline-cinnamic Acid Hybrids as Multifunctional Agents for Treatment of Alzheimer'S Disease, *Bioorg. Chem.*, 2020, **99**, 103844.

28 I. Pachón-Angona, B. Refouvelet, R. Andrýs, H. Martin, L. Vincent, I. Iriepa and I. Moraleda, Donepezil+ chromone+ melatonin hybrids as promising agents for Alzheimer's disease therapy, *J. Enzyme Inhib. Med. Chem.*, 2019, **34**, 479–489.

29 S. Bhandari, A. Agrwal, V. Kasana, S. Tandon, Y. Boulaamane and M. Amal, β-amino carbonyl derivatives: Synthesis, Molecular Docking, ADMET, Molecular Dynamic and Herbicidal studies, *ChemistrySelect*, 2022, **7**(48), e202201572.